



**POLITECNICO  
MILANO 1863**

**SCUOLA DI INGEGNERIA INDUSTRIALE  
E DELL'INFORMAZIONE**

EXECUTIVE SUMMARY OF THE THESIS

## Nonlinear Model Predictive Control of a thermo-hydraulic plant: design and experiments

LAUREA MAGISTRALE IN AUTOMATION AND CONTROL ENGINEERING - INGEGNERIA  
DELL'AUTOMAZIONE

**Author: CLAUDIO ANDERIS**

**Advisor: PROF. ALESSIO LA BELLA**

**Co-advisor: PROF RICCARDO SCATTOLINI, ING. ANDREA CATALDO**

**Academic year: 2021-2022**

### 1. Introduction

This thesis concerns the modelling and control of an energy system, i.e. District Heating System (DHSs). In fact, with the European Union targets to reduce the use of fossil fuels by 2050, interest in DHSs has increased [3]. DHSs should cover at least 50% of the heating demand of most European countries by 2050, achieving additional 30% of energy savings in the heating sector with respect to 2015 [4].

District heating means a system of distance heating units that, through a network of water pipelines, transports the heat generated by large thermal plants to individual residential units for domestic heating. District heating reduces energy waste and has a lower environmental impact than traditional heating methods. Thus, it is clear how optimization of these systems is necessary to have better energy efficiency.

The case study investigated in this thesis is a scaled-down thermo-hydraulic experimental plant designed and built with the contribution of the National Research Council (CNR) which it can be regarded as a reproduction of a DHS Figure 1.

The aim of this work is to design a Model Predictive Control (MPC) algorithm to optimize the behaviour of the system. The peculiarity of this type of control lies in the fact that control actions are obtained as a result of an optimization problem and, thus, the possibility of introducing constraints on inputs, outputs and states.

In particular, the aim is to track temperature references in the plant, by optimizing the performance of control variables.



Figure 1: Test Plant

## 2. Process Plant

The experimental plant consists of two thermo-hydraulic circuits, primary and secondary, thermally coupled by a heat exchanger and the fluid used is water.

The primary circuit is composed of a thermal coated tank with a thermal power supplier inside, a flow-controlled pump, a by-pass system with controlled valves and thermal coated piping circuits used to connect the different process component, Figure 2.

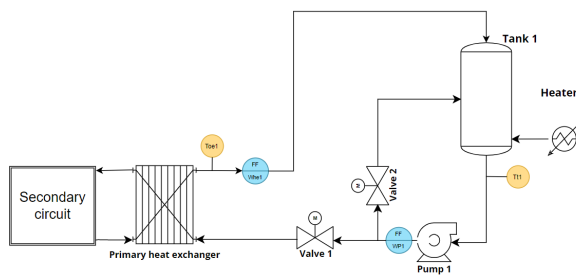


Figure 2: Primary Circuit

The secondary circuit is similar to the primary but with the difference that present two tanks without heaters inside them and is not coated. It also presents another component, secondary heat exchanger, that consists of a radiator into which the outlet water mass from the primary heat exchanger flows. Unlike the primary heat exchanger, there is only one water flow and thus the heat exchange takes place with the external environment. In addition, fans are mounted behind the exchanger so that there is the possibility of an additional cooling of the fluid, Figure 3.

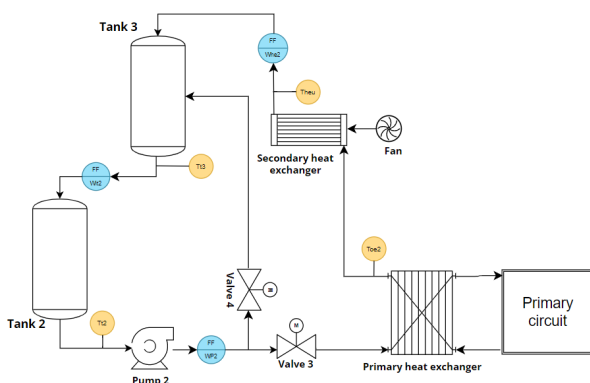


Figure 3: Secondary Circuit

There is an exchange of energy, in the form of heat exchange, between the primary circuit, generally at a higher temperature, towards the secondary. The water flow of both sides of the heat exchanger is ensured by the activation of the two pumps present, which are locally controlled to provide a constant flow rate. Thus, the heat transferred depends on the flow rates entering the exchanger, namely  $w_{he1}$  for the primary side and  $w_{he2}$  for the secondary side and each of this flow rates are controlled by a valve. There are other two valves, one per circuit, that constitute the bypass system and regulate the flow that goes directly back into the tanks.

## 3. Process Modelling

Having a model that well describes the dynamics of the system is fundamental because, first of all, it allows to develop a reliable simulator to analyse the control actions in simulation before applying them to the real plant. Then, one of the main ingredient for the type of control that will be designed, a Model Predictive Control (MPC), is a model that predicts the behavior of the system in order to generate the optimal sequence of control action.

The mathematical equations that govern the system have been derived from the laws of physics, in particular thermodynamics and fluid dynamics.

The following assumptions are made:

- the water is considered an incompressible fluid and its density is considered constant in each point of the hydraulic circuits;
- the temperatures of the flow rates are considered uniform along the pipes, so without losses to the environment;
- the pressures dynamics in the circuit are considered negligible.

Therefore, only the tanks and exchangers are analyzed and studied, while the pipes, pumps and valves, due to the assumptions just introduced, are not modeled in the final formulation. To recap the components that have been modeled by deriving their equations starting from the laws of thermodynamics and fluid dynamics are:

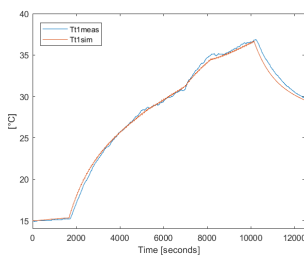
- The three Tanks present in the plant (Tank 1, Tank 2 and Tank3);
- The heater presents inside Tank 1;
- The primary heat exchanger.

Unlike the other components, the secondary heat exchanger model was identified as an ARX model using a black-box approach since the parameters of the fans and their model dynamics are not known. In particular, its modeling was carried out by identifying two models of the exchanger, one when the fans are off and one when are activated.

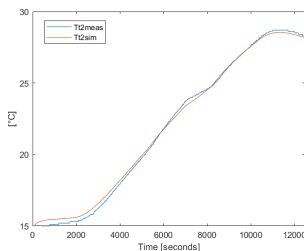
To summarize, the quantities of interest, i.e. the controlled variables, are the temperatures of the three present tanks,  $T_{T1}$ ,  $T_{T2}$  and  $T_{T3}$ , while the control variables are the two flow rate passing through the primary heat exchanger,  $w_{he1}$  and  $w_{he2}$ , and the power supplied by the heater inside Tank 1,  $P_e$ .

## 4. Software Development and Validation

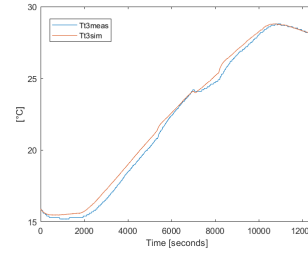
The mathematical equations found describing the process dynamics have been implemented in Simulink to obtain a simulated model. Thanks to the possibility to carry out tests on the real plant it was possible to validate the model by comparing the measured values with the simulations, obtaining the following good results



(a) Temperature  $T_{T1}$ : Simulation vs experiments



(b) Temperature  $T_{T2}$ : Simulation vs experiments



(c) Temperature  $T_{T3}$ : Simulation vs experiments

Figure 4: Comparison between simulation temperature trends and measured values

## 5. MPC Design and Simulation

A Model Predictive Control system (MPC) is designed with the aim to track temperature references. Since the model has nonlinearities, it is chosen to use a Nonlinear Model Predictive Control (NMPC) formulation [1] with the use of slack variables in order to have soft constraints on the states. For the inputs, it was chosen to weight the variation between subsequent time steps, including a constraint on the maximum possible variation. The formulation is the following

$$\begin{aligned}
 \min_{\Delta u} \quad & \sum_{i=0}^{N-1} (\|x(i+1|k) - x^{ref}\|_Q^2 + \|\Delta u(i+1|k)\|_R^2) + \rho s \\
 \text{s.t.} \quad & x(i+1|k) = f(x(i|k), u(i|k)), \quad i = 0, \dots, N-1, \\
 & x(0|k) = x_0, \\
 & U_{min} \leq U(k) \leq U_{max}, \\
 & \delta U_{min} \leq \Delta U(k) \leq \delta U_{max}, \\
 & X_{min} - sI \leq X(k) \leq X_{max} + sI, \\
 & s \geq 0
 \end{aligned}$$

The chosen states and inputs are

$$X(t) = \begin{bmatrix} h_{t2}(t) \\ h_{t3}(t) \\ T_{t1}(t) \\ T_{t2}(t) \\ T_{t3}(t) \end{bmatrix} \quad U(t) = \begin{bmatrix} P_e(t) \\ w_{he1}(t) \\ w_{he2}(t) \end{bmatrix} \quad (1)$$

where  $h_{t2}$  and  $h_{t3}$  are the water level inside the Tank 2 and Tank 3, respectively,  $T_{t1}$ ,  $T_{t2}$  and  $T_{t3}$  the temperatures of the three Tanks,  $P_e$  the power from the heater (The height in Tank 1 is fixed).

The choice of the weights of the Q matrix lies in the fact that the term corresponding to the controlled variables, namely  $T_{t1}$  and  $T_{t2}$ , is weighed

more heavily than the other states. The exclusion of the temperature of Tank 3 as a reference is due to the fact that, remembering the structure of the plant, Tank 2 and 3 are connected simply by a pipe and water flows by gravity, consequently the temperatures are related. The weights of the matrix  $R$  consider the different order of magnitude of the control inputs.

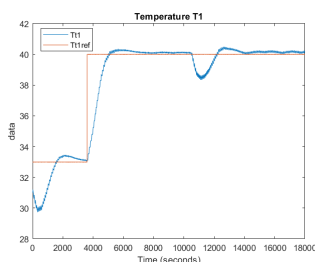
Since a nonlinear optimization problem needs to be solved, the NMPC was implemented using CasADI and IPOPT as solvers within Matlab [2].

### 5.1. Input Blocking

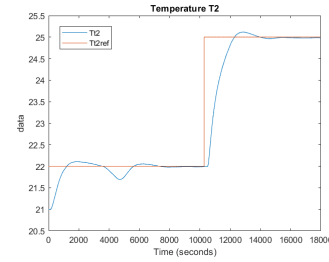
Given the slow dynamics of the system and the possibility of reducing computational time, the "Input blocking" strategy is introduced. This technique consists to reduce the degrees of freedom by fixing the input to be constant over several time- steps, in this way in the problem of optimization the variables are reduced and consequently its complexity leading to a reduction of the computational time. Instead of solving the optimal problem with respect to the input sequence  $U = [U_0, \dots, U_{N-1}]$ , the new problem can be restated in terms of solving for the optimal vector  $\hat{U} = [\hat{U}_0, \dots, \hat{U}_{v-1}]$  with  $v < N$ , number of input blocks. By reducing computational time it is also possible to increase the predictive horizon,  $N$ , and, being a system with a slow dynamics, it is possible to better predict its behavior.

### 5.2. Simulation Results

A test was executed with a predictive horizon of 30[min] and control variables held constant for 300[s], i.e. 5 minutes. The fans on the secondary exchanger where off.



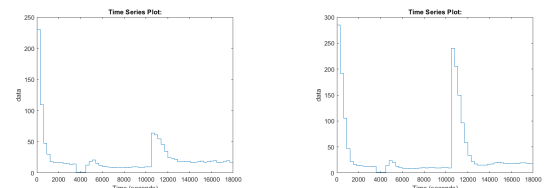
(a) Temperature Tank 1: Simulation results



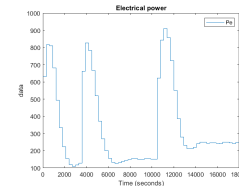
(b) Temperature Tank 2: Simulation results

Figure 5: Temperature trends in simulation

From the results obtained and shown in Figure 5 it can be seen how satisfactorily the references are followed and also the influences of the variations of the latter in the two circuits. The objective, however, is not just reference tracking, but, as mentioned above, a modulation of the control variables in such a way as to avoid large oscillations and variations so as to preserve actuator wearing and an efficient use of electrical power. The next figures show the trends of the three control variables.



(a) Primary Flow Rate  $w_{he1}$ : Simulation results (b) Secondary Flow Rate  $w_{he2}$ : Simulation results



(c) Electrical Power  $P_e$ : Simulation results

Figure 6: Control variables trends in simulation

## 6. MPC Implementation on the real system

Finally, the NMPC control system has been implemented and tested on the real plant. The optimization problem is computed in Matlab which interfaces with the Programmable Logic Controller (PLC) that manages everything related

to sensors and low level control architecture, i.e. the control of pumps and valves.

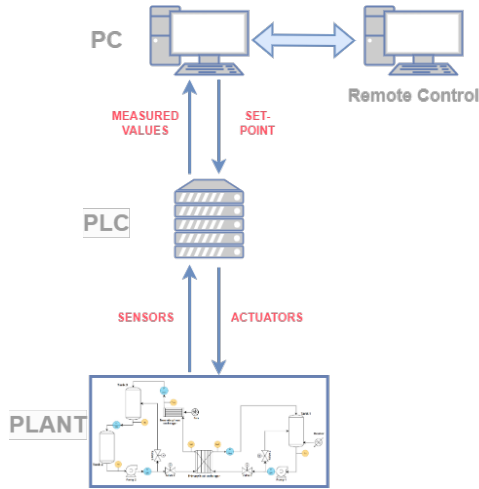


Figure 7: General scheme of the connection and flow of information of the entire system

In Figure 7 is represented the flow of information in the system. The entire procedure can be summarized in the following steps:

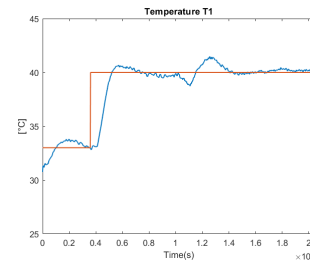
- The PLC receives data from the sensors on the plant, applies a filter action and send the new filtered values to Matlab
- Matlab receives the measured data from the PLC, executes the optimization procedure, generates the control actions and send the set-point values to PLC
- PLC controls the actuators in order to reach the set-points

The sensors on the plant are: five flow meters for the main flow rates and six temperature sensors that measure the temperatures of these five flow rates and one sensor for ambient temperature. The actuators, on the other hand, are the two pumps that provide continuous and constant flow in the two circuits and the two pairs of valves that constitute the bypass.

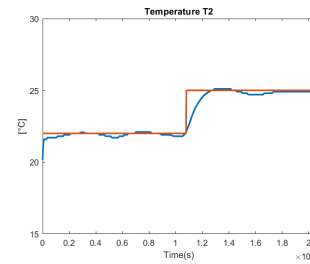
### 6.1. Test Results

The parameters used for the test, i.e. the predictive horizon, the run time of the MPC, the Q and R matrices and the various constraints, are the same as previously used in the simulation. Also for the scenario it has been chosen to use the same one, in this way it is also possible to verify the choices used in the modeling

phase comparing the results with those obtained in simulation.



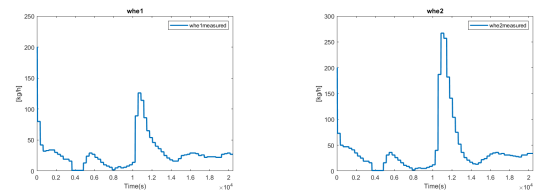
(a) Temperature Tank 1: Experimental test



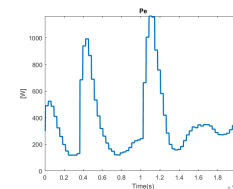
(b) Temperature Tank 2: Experimental test

Figure 8: Temperature trends in the real plant

Therefore, the similarity with the simulations shown in the Figure 5 appears evident, and for completeness it is appropriate to show the control variables as well.



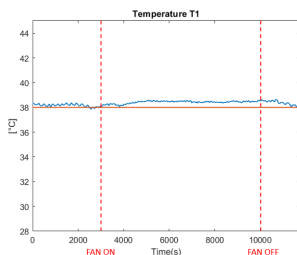
(a) Primary Flow Rate  $w_{he1}$ : Experimental test (b) Secondary Flow Rate  $w_{he2}$ : Experimental test



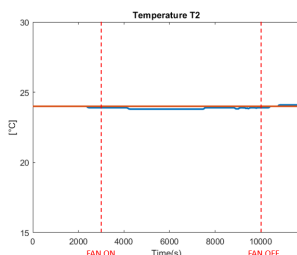
(c) Electrical Power  $P_e$ : Experimental test

Figure 9: Control variables trends in real plant

An additional test performed concerns the verification of the ARX model regarding the activation of the fans of the secondary heat exchanger. The test consists of keeping temperature references constant and turning on the fans during the experiment. Their activation is handled by a contactor and controlled through the PLC interface while in the MPC formulation, the switching from one model to the other is handled by a variable that can be assumed as a disturbance. Activation occurs at instant  $t=3000$  s while turning off at  $t=10000$  s.



(a) Temperature T1 trend with fan activation



(b) Temperature T2 trend with fan activation

Figure 10: Temperature trends with fan activation

As can be seen from both graphs in Figure 10, again the tracking remains very good, during the time interval when the fans are active it has only a difference of tenths of a degree from the reference. It could be slightly improved by a new identification of the ARX model when fans are active.

## 7. Conclusions

The aim of this work is to design a Model Predictive Control (MPC) algorithm to optimize the behaviour of the system. First, was derived a mathematical model that represents the dynamic behaviour of the process and then was

developed a Simulink model of the entire system.

Next, an NMPC optimization problem was formulated with the objective of tracking temperature references by penalizing variations in control variables.

Finally, the control scheme was implemented and tested in the actual plant obtaining good results.

Future developments regard the identification of the process model with a black-box system, like for example a Recursive Neural Networks (RNNs).

## References

- [1] F. Allgöwer, Rolf Findeisen, and Z.K. Nagy. Nonlinear model predictive control: From theory to application. *J. Chin. Inst. Chem. Engrs*, 35:299–315, 05 2004.
- [2] Joel A E Andersson, Joris Gillis, Greg Horn, James B Rawlings, and Moritz Diehl. CasADi – A software framework for nonlinear optimization and optimal control. *Mathematical Programming Computation*, 11(1):1–36, 2019.
- [3] Alessio La Bella and Ada Del Corno. Optimal management and data-based predictive control of district heating systems: The novate milanese experimental case-study. *Control Engineering Practice*, 132:105429, 2023.
- [4] Susana Paardekooper, Rasmus Søgaaard Lund, Brian Vad Mathiesen, Miguel Chang, Uni Reinert Petersen, Lars Grundahl, Andrei David, Jonas Dahlbæk, Ioannis Aristeidis Kapetanakis, Henrik Lund, Nis Bertelsen, Kenneth Hansen, David William Drysdale, and Urban Persson. *Heat Roadmap Europe 4: Quantifying the Impact of Low-Carbon Heating and Cooling Roadmaps*. Aalborg Universitetsforlag, October 2018.



**POLITECNICO**  
MILANO 1863

SCUOLA DI INGEGNERIA INDUSTRIALE  
E DELL'INFORMAZIONE

# Nonlinear Model Predictive Control of a thermo-hydraulic plant: design and experiments

TESI DI LAUREA MAGISTRALE IN  
AUTOMATION AND CONTROL ENGINEERING - INGEGNERIA  
DELL'AUTOMAZIONE

Author: **Claudio Anderis**

Student ID: 969046

Advisor: Prof. Alessio La Bella

Co-advisors: Prof. Riccardo Scattolini, Ing. Andrea Cataldo

Academic Year: 2021-22





*Ai miei nonni*



# Abstract

This work concerns the modeling and control of a scaled-down thermo-hydraulic plant which emulates a district heating system. The test plant, present in the IRMAP laboratory in Gorgonzola (MI), has been realized with the contribution of the National Research Council (CNR).

The aim of this thesis is to design and implement a Model Predictive Control (MPC) algorithm to optimize the behaviour of the system. The plant consists of two thermo-hydraulic circuits, primary and secondary, thermally coupled by a heat exchanger. The primary circuit involves the heat production, while the secondary the heat consumption by the user. First, starting from the physical laws of thermodynamics and fluid dynamics, a mathematical model is derived. Then, a simulation model of the plant is developed in Matlab (Simulink) validated by performing several tests on the real plant and comparing the obtained acquisitions with the simulations.

Then, the prediction control system is designed on the simulation model; given the nonlinearity of the model, a Nonlinear MPC (NMPC) formulation is chosen. Constraints on the states and inputs and the cost function used are introduced, and the prediction model is formulated. The control variables are managed in order to track temperature references, while reducing actuator usage and thermal energy. To enhance the computational performance, the "Input blocking" strategy is introduced. In the MPC optimization problem and discussed. The results obtained with different parameter choices are compared in simulations, eventually choosing the best design.

Finally, the implementation of the designed control scheme on the real plant is described and the results obtained are discussed.

**Keywords:** Model Predictive Control, Process Modeling, Energy Systems



# Abstract in lingua italiana

Questo lavoro riguarda la modellazione e il controllo di un impianto termoidraulico in scala ridotta che simula un sistema di teleriscaldamento. L'impianto di prova, presente nel laboratorio IRMAP di Gorgonzola (MI), è stato realizzato con il contributo del Consiglio Nazionale delle Ricerche (CNR).

Lo scopo di questa tesi è quello di progettare e implementare un algoritmo di Model Predictive Control (MPC) per ottimizzare il comportamento del sistema. L'impianto è costituito da due circuiti termoidraulici, primario e secondario, accoppiati termicamente da uno scambiatore di calore. Il circuito primario riguarda la produzione di calore, mentre il secondario il consumo di calore da parte dell'utente. Innanzitutto, partendo dalle leggi fisiche della termodinamica e della fluidodinamica, si ricava un modello matematico. Successivamente, viene sviluppato un modello di simulazione dell'impianto in Matlab (Simulink) convalidato eseguendo diversi test sull'impianto reale e confrontando le acquisizioni ottenute con le simulazioni.

Successivamente, il sistema di controllo predittivo viene progettato sul modello di simulazione; data la non linearità del modello, viene scelta una formulazione MPC non lineare (NMPC). Vengono introdotti i vincoli sugli stati e sugli ingressi e la funzione di costo utilizzata e viene formulato il modello di previsione. Le variabili di controllo sono gestite in modo da seguire i riferimenti di temperatura, riducendo al contempo l'utilizzo degli attuatori e l'energia termica. Per migliorare le prestazioni computazionali, viene introdotta e discussa la strategia di "Input blocking" nel problema di ottimizzazione MPC. I risultati ottenuti con diverse scelte di parametri vengono confrontati nelle simulazioni, scegliendo alla fine il progetto migliore.

Infine, viene descritta l'implementazione dello schema di controllo progettato sull'impianto reale e vengono discussi i risultati ottenuti.

**Parole chiave:** Model Predictive Control, Process Modeling, Energy Systems



# Contents

<b>Abstract</b>	<b>iii</b>
<b>Abstract in lingua italiana</b>	<b>v</b>
<b>Contents</b>	<b>vii</b>
<b>Introduction</b>	<b>1</b>
<b>1 Process Modelling</b>	<b>5</b>
1.1 Plant description . . . . .	5
1.1.1 Primary Circuit . . . . .	6
1.1.2 Secondary Circuit . . . . .	7
1.1.3 Modelling assumptions . . . . .	8
1.2 Preliminaries of Thermo-fluid dynamics . . . . .	9
1.2.1 Thermodynamics . . . . .	9
1.2.2 Conservation principles of fluid dynamics . . . . .	10
1.3 Thermo-hydraulic system modelling . . . . .	12
1.3.1 Primary Circuit . . . . .	12
1.3.2 Primary heat exchanger . . . . .	15
1.3.3 Secondary circuit . . . . .	17
1.4 Final Formulation . . . . .	23
1.5 Summary . . . . .	25
<b>2 Simulator development and validation</b>	<b>27</b>
2.1 Primary Circuit simulation model . . . . .	28
2.1.1 Tank 1 . . . . .	28
2.1.2 Heater . . . . .	28
2.2 Primary Heat Exchanger simulation model . . . . .	29
2.3 Secondary Circuit simulation model . . . . .	30

2.3.1	Tank 2 . . . . .	31
2.3.2	Tank 3 simulation model . . . . .	31
2.3.3	Secondary Heat Exchanger . . . . .	32
2.4	Simulation Model Validation . . . . .	36
<b>3</b>	<b>MPC Design and simulation</b>	<b>41</b>
3.1	MPC . . . . .	41
3.2	Nonlinear MPC . . . . .	42
3.2.1	NMPC formulation for tracking reference . . . . .	44
3.3	Case study: Implementation and Simulation . . . . .	45
3.3.1	Predictive Model of the Plant . . . . .	46
3.3.2	Simulation . . . . .	48
3.4	MPC Complexity Reduction . . . . .	52
3.4.1	Input Blocking (IB) . . . . .	53
<b>4</b>	<b>MPC Implementation in the real system</b>	<b>57</b>
4.1	Test Plant . . . . .	57
4.2	Components . . . . .	58
4.2.1	Programmable Logic Controller . . . . .	59
4.2.2	Sensors . . . . .	60
4.2.3	Actuators . . . . .	62
4.2.4	Secondary Heat Exchanger and Fans System . . . . .	65
4.3	Experiments . . . . .	66
4.3.1	MPC control . . . . .	66
	<b>Conclusions</b>	<b>73</b>
	<b>Bibliography</b>	<b>75</b>
	<b>List of Figures</b>	<b>77</b>
	<b>List of Tables</b>	<b>79</b>
	<b>Ringraziamenti</b>	<b>81</b>



# Introduction

## Motivation

In the last 50 years, due to the large use of fossil fuels, the concentration of carbon dioxide ( $CO_2$ ) in the atmosphere has been increasing from approximately 300 parts per million (ppm) to 414.7 ppm in 2021 [7]. This increasing pollution, which is very harmful to humans and the environment, is due to the fact that the constant increasing energy demand is today provided for 84.32 % by fossil fuels, 4.27 % by nuclear power, and the remainder by renewable sources [16]. With the target by the European Union to reduce the use of fossil fuels by 2050, the ecological transition is initiated, specifically focused on the reduction of fossil fuel based power generation in favor of renewable sources and the more efficient and cost-effective energy systems. Given this context, this thesis focuses on the District Heating Systems (DHSs) [9], which should cover at least 50% of the heating demand of most European countries by 2050, achieving additional 30% of energy savings in the heating sector with respect to 2015 [14]. District heating means a system of distance heating units. Through a network of water pipelines, it transports the heat generated by thermal plants to individual residential units for domestic heating. District heating reduces energy waste and has a lower environmental impact than traditional heating methods. Thus, it is clear how optimization of these systems is necessary to have better energy efficiency and make an important contribution to the ecological transition. The so called "standard" control methods, such as PID control, are unable to meet these demands, and so the necessity to design "advanced control methods" has arisen. Model Predictive Control, that is by far the most popular one, uses a model of the process to make predictions about its behavior and then find the control action to be applied to the system by minimizing a cost function, so, one of its main advantages that differentiate it from other methods is that control actions are obtained as a result of an optimization problem and, thus, the possibility of introducing constraints on inputs, outputs and states. The more accurate a model is to reality, the better the results achieved, and so the modeling phase is one of the most crucial part of these methods.

## Case of study

Back to DHSs, as they are large-scale complex systems, a direct study of them would require a lot of time and resources, so it is sometimes convenient to design smaller plants in order to study, implement and verify control systems more quickly than in a real ones of larger size. For this purpose, a scaled-down model of a thermo-hydraulic system has been designed in collaboration with National Research Council (CNR), located in IRMAP Laboratory present in Gorgonzola (MI)<sup>1</sup>. This is the subject of the study of this thesis, and a photo of it is shown in Figure 1. A more detailed description will be given in the dedicated chapter.



Figure 1: Test Plant located at IRMAP Laboratory

The plant consists of two circuits thermally coupled through a heat exchanger, and thus an exchange of energy takes place. The primary circuit, which can be distinguished in the photo by the fact that it is coated, is where the water is heated, partly due to the presence of a resistor placed inside the primary tank. This circuit, then, through a heat exchanger placed in the center, transfers heat to the secondary circuit, which has two not insulated tanks. Various actuators, such as pumps and valves, are present to manage the flow rates of the entire system.

---

<sup>1</sup>IRMAP SERVICE srl (Istituto di Ricerca sulla Manutenzione e Produzione), entity that collaborates with STIIMA-CNR in activities to develop industrial applications and services for industry, research and education, including through the use of APRs (Remotely Piloted Aircraft).

The sequence of steps carried out throughout the thesis work can be divided into four main phases:

- Process Modeling
- Simulator development and validation of the model with the plant
- MPC control design and tests applied to the simulated model
- Implementation of the MPC control to the real plant and tests

The control system was developed in Matlab & Simulink environment. The sensors, i.e., the acquisition of the data of interest, and the low-level control actions, i.e., control of the valves and pumps, are all handled by a Programmable Logic Controller (PLC) that interfaces with Matlab. The overall control scheme is shown in Figure 2. The thesis focuses mainly on the modelling of the plant and the design of the MPC type control system respect to PLC implementation.

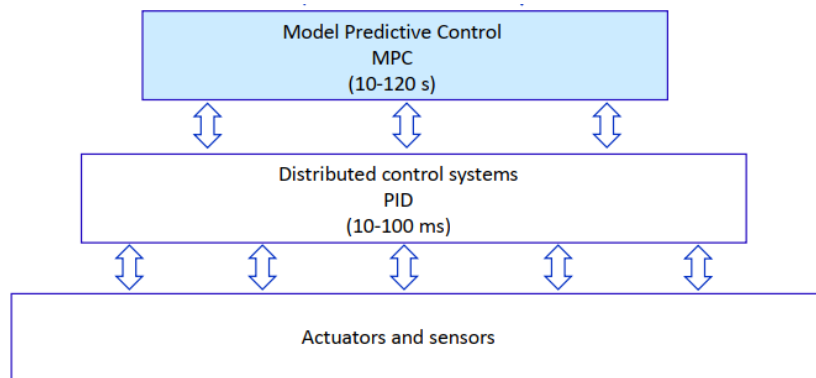


Figure 2: Control Scheme. The lower two blocks are handled by the PLC while the upper block is implemented in Matlab.

The goal of the MPC is to control the operating temperature of the primary circuit, by managing the various flow rates through valve regulation and thus manage how much heat to release to the secondary, but, however, also keeping the temperatures of the secondary circuit under control.

## Thesis structure

The structure of the thesis follows the sequence of work steps introduced before and each chapter coincides with one of them. The thesis is organized as follows:

- **Chapter 1:** Initially, a description of the plant and of its working principle is provided. Then, the physical equations governing the system are derived from physical laws and the modeling of each components is discussed.
- **Chapter 2:** Starting from the equations found in the previous chapter, the simulator development and its validation with real data is discussed.
- **Chapter 3:** The MPC regulation system is designed and tested in simulation.
- **Chapter 4:** The main components of the plant are described in more detail, and the designed MPC is tested on the real system. The obtained results and control performance are discussed.
- **Conclusions:** A brief recap is given on the work done by commenting on the results obtained and discussing possible future developments.

# 1 | Process Modelling

In this chapter, the real plant is described and the mathematical equations modelling its dynamics are formulated. This will be explained in the following paragraphs.

## 1.1. Plant description

Before presenting the model, the components and the entire process are described. A general scheme of the whole system, with the main components, is depicted in Figure 1.1.

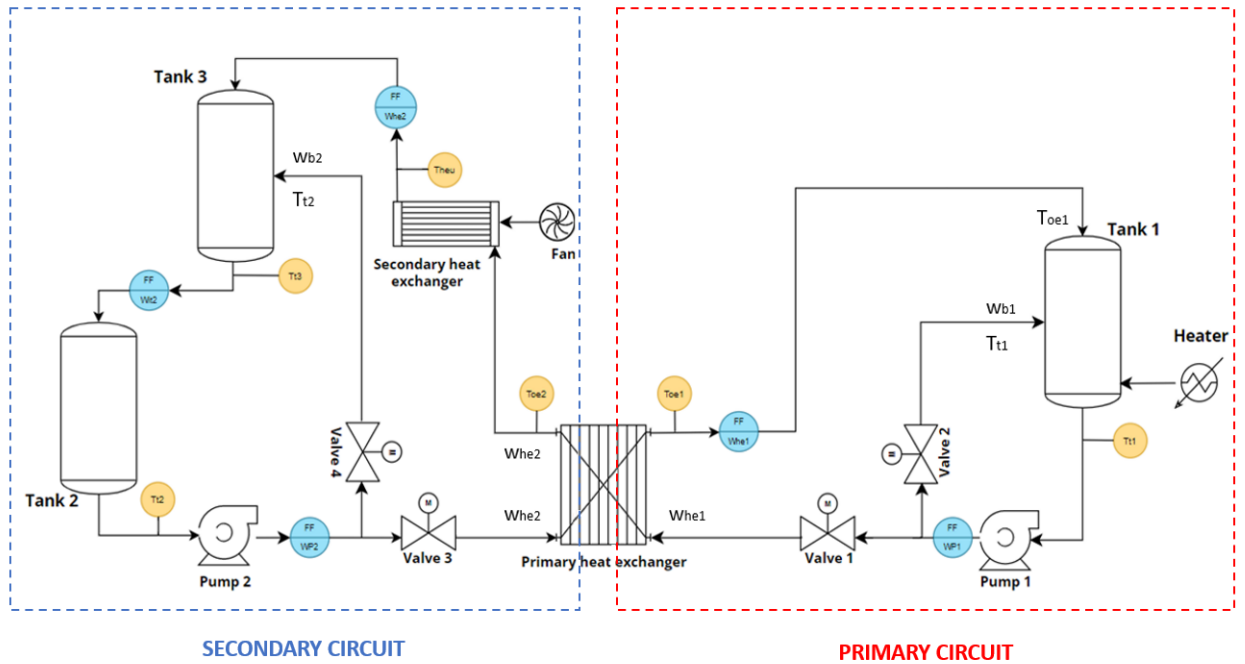


Figure 1.1: Scheme of the plant

From the diagram, it can be seen that the whole system can be decomposed into two circuits, primary and secondary, thermally coupled by the primary heat exchanger. Through the latter, the primary circuit transfers heat to the secondary one. In fact, a heater is present in Tank 1 of the primary circuit, whereas the load (i.e. the secondary heat ex-

changer) is placed in the secondary circuit. The following subsections will describe in detail the two circuits with their components and sensors. The listed sensors and actuators in the system respectively send and receive signals from a Programmable Logic Controller (PLC). The PLC communicates with the Matlab and Simulink through which it is possible to act on plant control variables and collect data provided by sensors.

### 1.1.1. Primary Circuit

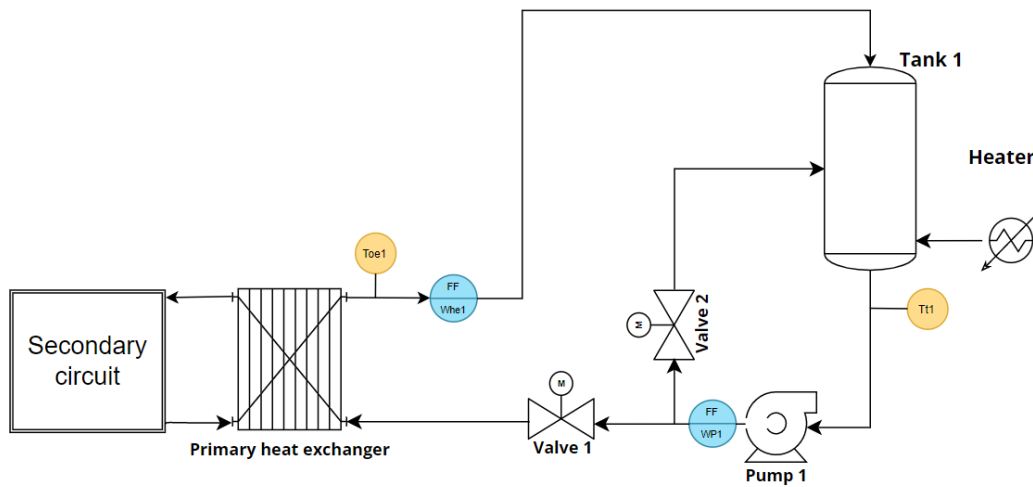


Figure 1.2: Scheme of the Primary circuit

The primary circuit, as shown in Figure 1.2, is composed of a thermal coated tank (Tank 1) with a thermal power supplier inside, a flow-controlled pump (Pump1), a by-pass system with controlled valves (Valve 1 and 2), a heat exchanger and thermal coated piping circuits used to connect the different process components. Being the tank and the pipes thermal coated, the heat transfer with the external environment is negligible and the water temperature is constant along the piping circuit. The sensors present are:

- **Tt1**: Temperature sensor which measures the temperature at the outlet of Tank 1;
- **Toe1**: Temperature sensor which measures the temperature at the outlet of the primary heat exchanger, primary circuit side;
- **wp1**: Flowmeter measuring the flow rate at the pump 1 outlet;
- **whe1**: Flowmeter measuring the flow rate at the primary heat exchanger outlet;

### 1.1.2. Secondary Circuit

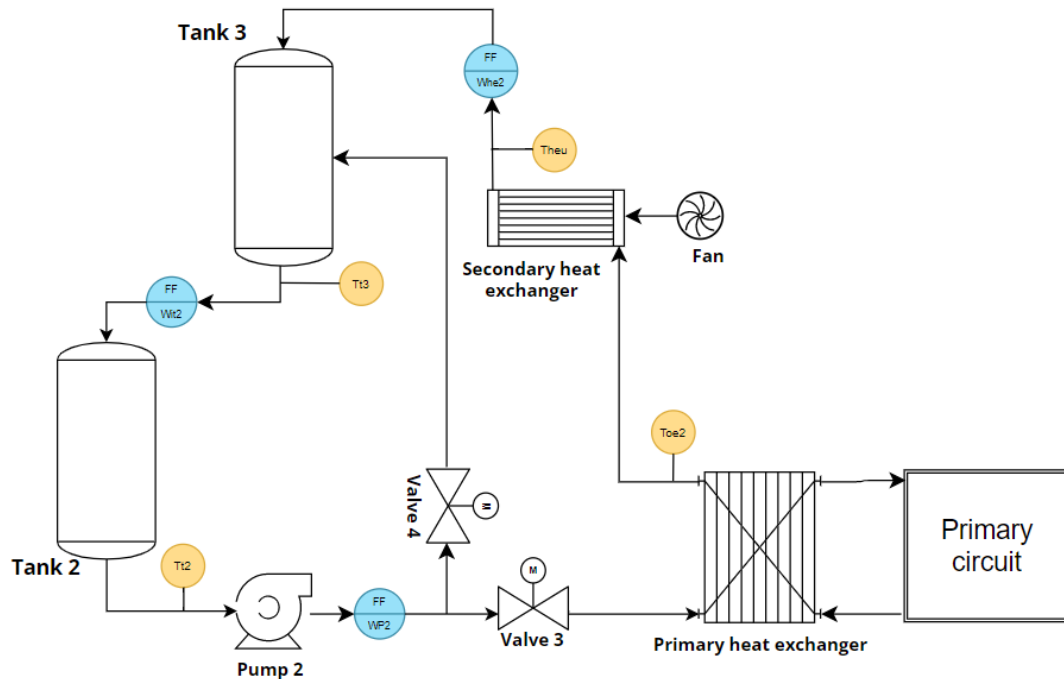


Figure 1.3: Scheme of Secondary circuit

The secondary circuit, shown in Figure 1.3 has some differences with the primary circuit. The first difference is the presence of two tanks, Tank 2 and Tank 3, but without an internal heater. The other difference is the presence of an additional heat exchanger which cools the water through local fans. In this circuit, the pipes and the tanks are not coated but the water flow value is such that the interval time needed to cover the piping length is negligible with respect to the tank temperature dynamic. The sensors present are:

- **Tt2**: Temperature sensor which measures the temperature at the outlet of Tank 2;
- **Tt3**: Temperature sensor which measures the temperature at the outlet of Tank 3;
- **Toe2**: Temperature sensor which measures the temperature at the outlet of the primary heat exchanger, secondary circuit side;
- **Theu**: Temperature sensor which measures the temperature at the outlet of the secondary heat exchanger;
- **wp2**: Flowmeter measuring the flow rate at the pump 2 outlet;
- **whe2**: Flowmeter measuring the flow rate at the secondary heat exchanger outlet;

- **wit2:** Flowmeter measuring the flow rate at the Tank 3 outlet;

The main energy exchange occurs through the primary heat exchanger, as there is a heat transfer from the primary circuit, generally at higher temperature, to the secondary circuit. The water flows on both sides of the heat exchanger are ensured by the activation of the two pumps present, which are locally controlled to provide a constant flow rate. Thus, the heat transferred depends also on the flow rates entering the exchanger, namely  $w_{he1}$  for the primary side and  $w_{he2}$  for the secondary side. These two flows are controlled by the opening and closing of Valve 1 (primary circuit) and Valve 3 (secondary circuit), respectively. As can be seen from the diagrams there are two other valves, Valve 2 (primary circuit) and Valve 4 (secondary circuit), these constitute the bypass system and regulate the flow that goes directly back into the tanks. The valves are controlled locally by PID controllers so as to follow the reference.

Another quantity that contributes to the energy exchange is the temperature at the inlet of the primary-side exchanger. This temperature, which corresponds to the outlet temperature from Tank 1 since the primary circuit is thermally isolated, can be increased through the electrical resistance in the tank. On the other hand, the temperature of the water in tank 2 and tank 3, varies only according to the heat exchange with the primary circuit and the cooling due to the secondary heat exchanger located immediately after the primary one.

### 1.1.3. Modelling assumptions

There are two methods to develop the mathematical model of the system:

- **Physical models:** derived from knowledge of the physics of the process, and then through mass, energy and momentum balance;
- **Data-driven models:** when there is no knowledge of the physics governing the system but a model is found through quantitative observations, measurements and experiments.

The physical laws governing most of the components are well known, and so with the use of these, the mathematical equations will be found. The only exception is the modeling of the secondary heat exchanger, for which, as will be explained in the dedicated section, an identification model was found. But before entering into the discussion, some assumptions are made:

- the water is considered an incompressible fluid and its density is considered constant in each point of the hydraulic circuits;



- due to the small dimension of the plant, the temperatures of the flow rates are considered uniform along the pipes, so without losses to the environment;
- the pumps present always operate at their nominal conditions, i.e., around a flow rate value of  $0,111[\frac{Kg}{s}]$ , that is,  $400[\frac{Kg}{h}]$ .
- pipes have limited length with dynamics negligible with respect to the tanks ones;
- the pressures modelling in the circuit is not considered because most of the pipes are short and with reduced head losses;

Therefore, only the tanks and exchangers will be analyzed and studied, while the pipes, pumps and valves, due to the assumptions just introduced, will not be modeled in the final plant model.

## 1.2. Preliminaries of Thermo-fluid dynamics

### 1.2.1. Thermodynamics

Thermodynamics studies physical phenomena in which energy exchange in the form of heat and mechanical work takes place. A thermodynamic system is a finite region of space (or finite amount of matter) divisible, ideally or not by the surrounding environment. Thermodynamic systems can be:

- **Open:** exchange energy (thermal and mechanical) and mass with the external environment.
- **Closed:** exchange only energy with the outside.
- **Insulated:** exchange neither energy nor mass with the outside world.

In the plant, all components are considered as open systems.

### First principle of thermodynamics in open systems

The first principle of thermodynamics in open systems can be expressed as [13]:

$$\frac{dE_{tot}(t)}{dt} = \delta L + \delta Q + \frac{dE_{tot,in}(t)}{dt} - \frac{dE_{tot,out}(t)}{dt} + \delta L_i - \delta L_o \quad (1.1)$$

In eq. (1.1) the quantity:

$$E_{tot} = \int_V \rho \left( e + \frac{1}{2} \cdot u^2 + g \cdot z \right) dV \quad (1.2)$$

is the total energy contained in volume V, the sum of internal, kinetic and potential energy,  $\rho$  is the flow density,  $e$  the internal energy,  $u$  the flow speed,  $g$  the gravitational coefficient and  $z$  the fluid level in the volume. Eq. (1.1) then expresses the time variation of  $E_{tot}$  as the result of the following contributions:

- $\delta L$  and  $\delta Q$  are the work and heat absorbed per unit time.
- $\frac{dE_{tot,in}(t)}{dt}$ ,  $\frac{dE_{tot,out}(t)}{dt}$  are the energies with which a fluid enters and leaves the system.
- $\delta L_i, \delta L_o$  is work done by the mass entering and leaving the system.

### 1.2.2. Conservation principles of fluid dynamics

Fluid dynamics deals with the study of fluid motion and its causes [8]. Regarding the study of the balancing equation of a quantity, two models are considered:

- **0-dimensional models:** the volume being considered has no spatial dimensions, all variables are just functions of time.
- **1-dimensional models:** variables can be a function of spatial dimensions.

In the plant, all components are described by 0-dimensional models.

### Balance equation (0-dimensional models)

#### Mass balance

The mass balance equation is:

$$\frac{d}{dt} \int_V \rho(x,t) dV = w_i(t) - w_o(t) \quad (1.3)$$

Where  $\rho(x,t)$  is the flow density,  $w_i(t)$  and  $w_o(t)$  are respectively the flow rate into and out of the system. If a 0-dimensional model is considered,  $\rho$  does not depend on spatial dimensions and eq. (1.3) becomes:

$$\frac{d}{dt} \rho(t) \int_V dV = \frac{dm(t)}{dt} = w_i(t) - w_o(t) \quad (1.4)$$

Where  $m(t)$  is the mass of the volume V.

## Energy Balance

The principle of conservation of energy referred to an infinitesimal interval  $dt$  is the first principle of thermodynamics for open systems, (1.1), where:

$$\left\{ \begin{array}{l} \delta Q = \Phi(t)dt, \quad \text{with } \Phi(t) \text{ thermal power,} \\ \delta L = \Psi(t)dt, \quad \text{with } \Psi(t) \text{ mechanical power,} \\ dE_{ti} = dm_i \cdot e_{ti} = dm_i \cdot \left( e_i + \frac{u_i^2}{2} + g \cdot z_i \right), \\ dE_{to} = dm_o \cdot e_{to} = dm_o \cdot \left( e_o + \frac{u_o^2}{2} + g \cdot z_o \right), \\ \delta L_i = p_i \cdot dV_i, \\ \delta L_o = p_o \cdot dV_o, \end{array} \right. \quad (1.5)$$

Remembering that  $w = \frac{dm}{dt}$ ,  $dV = \frac{dm}{\rho}$  and  $u = \frac{w}{\rho \cdot A}$  the final energy balance equation becomes:

$$\frac{dE_{tot}(t)}{dt} = \delta L + \delta Q + w_i(t) \left( e_i + \frac{u_i^2}{2} + g \cdot z_i + \frac{p_i}{\rho_i} \right) - w_o(t) \left( e_o + \frac{u_o^2}{2} + g \cdot z_o + \frac{p_o}{\rho_o} \right) \quad (1.6)$$

Noting that  $h = e + \frac{p}{\rho}$ , i.e. the specific enthalpy, the eq. (1.6) becomes:

$$\frac{dE_{tot}(t)}{dt} = \delta L + \delta Q + w_i(t) \left( h_i + \frac{u_i^2}{2} + g \cdot z_i \right) - w_o(t) \left( h_o + \frac{u_o^2}{2} + g \cdot z_o \right) \quad (1.7)$$

It's important to notice that, in our case, kinetic and potential components can be neglected from the balance equation. This is because the fluid speed is negligible and the fluid level does not change significantly. Moreover, if the fluid is water,  $h = e + \frac{p}{\rho} \simeq e = c_w \cdot T$ , so the balance equation becomes:

$$\frac{dE_{tot}(t)}{dt} = \delta L + \delta Q + w_i(t) \cdot c_w \cdot T_i - w_o(t) \cdot c_w \cdot T_o \quad (1.8)$$

And the energy is:

$$E_{tot}(t) = m \cdot e(t) = m \cdot c_w \cdot T(t) = c_w \cdot \rho \cdot A \cdot h(t) \cdot T(t) \quad (1.9)$$

Recalling that  $c_w$  is the water specific heat,  $\rho$  is the water density, assumed to be constant,  $h(t)$  the fluid level and finally  $T$  is the water temperature.

## 1.3. Thermo-hydraulic system modelling

### 1.3.1. Primary Circuit

#### Tank 1

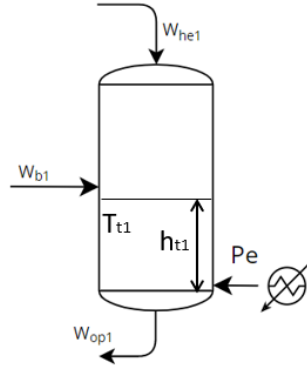


Figure 1.4: Tank 1 schematic

#### Mass balance

Tank 1, as shown in the Figure 1.4, has two inlets, one from the bypass and one from the heat exchanger, and one outlet. Hence, the mass balance is described by eq. (1.10):

$$\frac{dm_1(t)}{dt} = w_{b1}(t) + w_{he1}(t) - w_{op1}(t) \quad (1.10)$$

then, since the water mass is

$$m(t) = \rho \cdot A_{t1} \cdot h_{t1}(t) \quad (1.11)$$

it follows that:

$$\frac{dh_{t1}(t)}{dt} = \frac{1}{\rho \cdot A_{t1}} \cdot (w_{b1}(t) + w_{he1}(t) - w_{op1}(t)) \quad (1.12)$$

where  $h_{t1}(t)$  is the water level in the tank,  $\rho$  and  $A_{t1}$  are the water density and the tank section,  $w_{b1}(t)$  is the inlet mass flow from by-pass 1,  $w_{he1}(t)$  is the inlet mass flow from the primary heat exchanger and  $w_{op1}(t)$  is the outlet mass flow.

Since the hydraulic circuit is a closed loop, it holds that

$$w_{b1}(t) + w_{he1}(t) = w_{op1}(t) \quad (1.13)$$

so eq. (1.12) becomes

$$\frac{dh_{t1}(t)}{dt} = 0 \quad (1.14)$$

that means  $h_{t1}(t) = h_{t1}$ . In other words the water level in tank  $T_1$  is constant and the water mass in the tank is  $m_{1w} = \rho \cdot A_{t1} \cdot h_{t1}$ .

### Energy balance

Recalling the power balance equation for liquids, see (1.8), it follows that

$$\frac{dE_{tot}(t)}{dt} = P_e(t) + w_{b1}(t) \cdot c_w \cdot T_{oe1}(t) + w_{he1}(t) \cdot c_w \cdot T_{t1}(t) - w_{op1}(t) \cdot c_w \cdot T_{t1}(t) \quad (1.15)$$

where  $P_e(t)$  is the power from the heater,  $T_{oe1}$  is the temperature of the inlet water flow  $w_{he1}(t)$ ,  $T_{t1}$  the temperature of inlet water flow  $w_{b1}(t)$ . The outlet water flow is  $w_{op1}(t)$ , where the temperature of the water leaving the tank is considered to be equal to the temperature inside it.

Then, substituting (1.9) in (1.15) we obtain:

$$\begin{aligned} c_w \cdot \rho_w \cdot A_{t1} \cdot \left[ T_{t1} \cdot \frac{dh_{t1}(t)}{dt} + h_{t1} \cdot \frac{dT_{t1}(t)}{dt} \right] = \\ = P_e(t) + c_w \cdot [w_{b1}(t) \cdot T_{t1}(t) + w_{he1}(t) \cdot T_{oe1}(t) - w_{op1}(t) \cdot T_{t1}(t)] \end{aligned} \quad (1.16)$$

Finally, recalling (1.12), (1.10) and omitting a few steps, the temperature dynamics inside the tank is described by the following equation

$$\frac{dT_{t1}(t)}{dt} = \frac{P_e(t)}{m \cdot c_w} + \frac{w_{he1}(t)}{m} \cdot (T_{oe1}(t) - T_{t1}(t)) \quad (1.17)$$

Interestingly, only the contribution due to the inflow from the primary exchanger appears in the final balance. This is because by substituting the mass balance into the equation (1.16), the contributions due to the flow rate from the bypass and that at the tank outlet cancel out. The outflow rate is the sum of the bypass flow rate and the flow rate passing through the exchanger. Since  $w_{b1}$  enters and exits the tank through the bypass with the same temperature this makes no contribution to the energy balance and therefore cancels out. The only flow rate that varies its inlet and outlet temperature and is therefore to be considered in the balance is  $w_{he1}$ .

Another important observation is that in eq. (1.17), the mass  $m$  considered is only the water one and thus neglecting the mass of the metal wall. To justify this approximation, an analysis was performed that concerns the calculation of the time interval required to reach a reference water temperature with and without modelling the metal wall. In this

way it can be checked whether it is possible to simplify the thermal modelling equation. A constant water level of 15 cm is considered in the analysis. With a diameter of the Tank  $d$  equal to 50 cm, the total water mass  $m_{1w}$  is 29 kg, while the metal mass  $m_{1m}$  is equal to 10 kg, so one third of the total mass, thus the metal mass is not negligible with respect to the water one, but, the specific heat of the water is equal to  $4186[\frac{J}{kg^{\circ}C}]$  and of the metal is equal to  $450[\frac{J}{kg^{\circ}C}]$ . The test consists of calculating the time interval required for the water temperature inside Tank 1 to reach a temperature  $T_f = 50[^{\circ}C]$  from an initial temperature  $T_{amb} = 20[^{\circ}C]$  with  $P_e = 2200[W]$ , first modelling only water mass and then also with metal mass. Starting from the energy balance equation within the Tank,(1.17), considering only the contribution due to the electrical power of the resistor (i.e.,  $w_{he1} = 0$

$$\frac{T_f - T_{amb}}{\Delta t} = \frac{P_e}{m \cdot c_w} \quad (1.18)$$

it follows that

$$\Delta t = \frac{(T_f - T_{amb}) \cdot m \cdot c_w}{P_e} \simeq 1681[s] \simeq 0.47[h] \quad (1.19)$$

with the thermal power  $P_e = 2200[W]$ , the maximum value.

Taking the metal mass into account, since the tank is thermal coated the heat convection with the external environment can be neglected. Because of the high thermal conductivity between water and metal and its small thickness, it can be assumed that the water and metal temperature to be equal at any time instant. In this case, it would follow that

$$\Delta t' = \frac{(T_f - T_{amb}) \cdot (m \cdot c_w + m_{1m} \cdot c_m)}{P_e} \simeq 1742[s] \simeq 0.48[h] \quad (1.20)$$

So, since the two time intervals are almost the same, the metal heating can be neglected in the tank thermal energy modelling.

## Heater

The heater system consists of a pair of electrical resistances placed inside the tank. Since the power provided by the heater can be only null or equal to the maximum power, i.e., 2200 W, the power has been modulated by means of "Pulse-Width Modulation" technique (PWM) in order to have the desired  $P_{em}(t)$ . This is done by the program implemented

in the PLC, which receives the setpoint value provided by the control system and then, through PWM modulation, manages the switching on and off of the electrical current resistor. In particular, a fixed  $T_{on}$  is kept at 25 s and the program calculates the time  $T_{off}$  with the following formula:

$$T_{off} = \left(\frac{P_e}{S_p} - 1\right) \cdot T_{on} \quad (1.21)$$

Where  $P_e$  is the maximum power, 2200 W, and  $S_p$  is the required power setpoint.

### 1.3.2. Primary heat exchanger

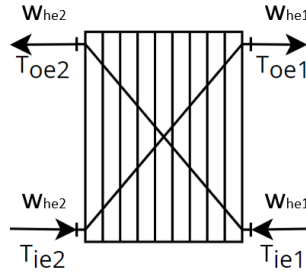


Figure 1.5: Primary heat exchanger schematic

The primary heat exchanger is the element that couples the two hydraulic circuits. A heat exchanger is a equipment in which heat is transferred from a hot fluid, i.e., at a higher temperature, to a cold fluid, i.e., at a lower temperature. There are various types of heat exchanger models; the one used in the system is a concentric tube heat exchanger. This means that the two fluids pass inside two tubes placed in contact with each other so as to perform heat exchange. In this case the exchanger is mounted in counter-current configuration, in which the two fluids are made to flow in opposite directions. Since also this element is thermally coated, no leakage with the external environment is considered. Under the assumption that water is an incompressible fluid, the inlet and outlet mass flow remain constant. The thermal energy exchanged between the two fluid, indicate as  $Q_{12}$ , is governed by the following equations

$$\frac{dQ_{12}(t)}{dt} = c_w \cdot w_{he1}(t) \cdot (T_{t1}(t) - T_{oe1}(t)) \quad (1.22)$$

$$\frac{dQ_{12}(t)}{dt} = c_w \cdot w_{he2}(t) \cdot (T_{oe2}(t) - T_{t2}(t)) \quad (1.23)$$

with  $w_{he1}(t)$  and  $w_{he2}(t)$  are the mass flow rates,  $T_{t1}(t)$  and  $T_{oe1}(t)$ ,  $T_{t2}(t)$  and  $T_{oe2}(t)$  respectively the inlet and outlet temperatures, see Figure 1.5. Then, in order to represent the internal global heat exchange, the  $\epsilon$ -NTU method is used.

### $\epsilon$ -NTU method

This method is based on a dimensionless parameter called "effectiveness of the heat exchanger heat," defined by the relation:

$$\epsilon = \frac{\dot{Q}_{12}}{\dot{Q}_{max}} \quad (1.24)$$

When the  $\dot{Q}$  notation is used to indicate the derivative with respect to time of the quantity  $Q$ . In particular,

- $\dot{Q}_{12}$  is the power actually exchanged by the heat exchanger. This power is calculated through the formulas (1.25):

$$\dot{Q}_{12} = c_w \cdot w_{he1}(t) \cdot (T_{t1}(t) - T_{oe1}(t)) = c_w \cdot w_{he2}(t) \cdot (T_{oe2}(t) - T_{t2}(t)) \quad (1.25)$$

- $\dot{Q}_{max}$  is the maximum value of theoretically exchangeable heat power. This power can be achieved only in a counterflow exchanger of infinite length. The general formula for calculating it is:

$$\dot{Q}_{max} = C_{min} \cdot (T_{ie1} - T_{ie2}) \quad (1.26)$$

where  $C_{min}$  is the minimum value between  $c_w \cdot w_{he1}(t)$  and  $c_w \cdot w_{he2}(t)$ , i.e.,  $C_{min} = c_w \cdot \min(w_{he1}, w_{he2})$ .

Knowledge of the effectiveness of the exchanger as a known parameter thus makes it possible to calculate the heat output actually exchanged without having to determine the outlet temperatures of the hot and cold fluids (i.e.,  $T_{oe1}$  and  $T_{oe2}$ ). It follows that

$$\dot{Q}_{12} = \epsilon \cdot \dot{Q}_{max} = \epsilon \cdot C_{min} \cdot (T_{ie1} - T_{ie2}) \quad (1.27)$$

The value of the effectiveness  $\epsilon$  depends on the geometry of the exchanger itself, and its type, and can be found on special tables; however, it is also possible to determine the



value of  $\epsilon$  analytically. For a countercurrent exchanger, the formula is [12]:

$$\epsilon = \frac{1 - \exp\left[-\frac{K_{12} \cdot A}{C_{min}(1 - \frac{C_{min}}{C_{max}})}\right]}{1 - \frac{C_{min}}{C_{max}} \cdot \exp\left[-\frac{K_{12} \cdot A}{C_{min}(1 - \frac{C_{min}}{C_{max}})}\right]} \quad (1.28)$$

where  $K_{12}$  is the global heat exchanger coefficient and  $A$  the cross-sectional area of the tube.

Introducing the parameter:

- **Capacity ratio:**  $C_r = \frac{C_{min}}{C_{max}}$ ,  $0 \leq C_r \leq 1$
- **NTU:** Number of Transfer Units:  $NTU = \frac{K_{12} \cdot A}{C_{min}}$

equation (1.28) becomes:

$$\epsilon = \frac{1 - \exp[-NTU(1 - C_r)]}{1 - C_r \exp[-NTU(1 - C_r)]} \quad (1.29)$$

If  $C_r = 1$  ( $C_{min} = C_{max}$ ), it follows that

$$\epsilon = \frac{NTU}{1 - NTU} \quad (1.30)$$

### 1.3.3. Secondary circuit

#### Tank 2

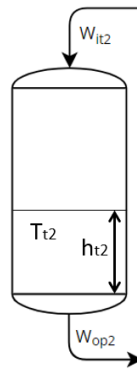


Figure 1.6: Tank 2 schematic

Differently from Tank 1, Tank 2 is not coated, does not have an internal heater and the water level inside may vary. Its modelling is represented in the following.

### Mass Balance

The mass balance is described by eq. (1.31):

$$\frac{dh_{t2}(t)}{dt} = \frac{1}{\rho \cdot A_{t2}} \cdot (w_{it2}(t) - w_{op2}(t)) \quad (1.31)$$

where  $h_{t2}(t)$  is the water level in the tank,  $A_{t2}$  the tank section,  $w_{it2}(t)$  and  $w_{op2}(t)$  the inlet and outlet mass flow, respectively.

### Energy balance

Similar to what has already been discussed in (1.3.1), but with no power from the heater, the energy balance in Tank 2 leads to the following eq.:

$$\frac{dE_{tot}(t)}{dt} = w_{it2}(t) \cdot c_w \cdot T_{t3}(t) - w_{op2}(t) \cdot c_w \cdot T_{t2}(t) - \beta_2 \cdot (T_{t2}(t) - T_{amb}(t)) \quad (1.32)$$

In this case, convection loss due to heat exchange with the environment is added to the balance. This is because, unlike what was seen for Tank 1, Tank 2 is not thermally coated. The coefficient  $\beta_2$  can be found empirically. Finally, recalling (1.31) and omitting a few steps, the temperature dynamics inside the tank is described by the following equation:

$$\frac{dT_{t2}(t)}{dt} = \frac{1}{\rho \cdot A_{t2} \cdot h_{t2}(t)} \cdot [w_{it2}(t) \cdot (T_{t3}(t) - T_{t2}(t)) - \beta_2 \cdot (T_{t2}(t) - T_{amb}(t))] \quad (1.33)$$

Again, as in Tank 1, the only contribution present is that due to the inlet flow rate.

## Tank 3

Tank 3 has a similar structure to Tank 2, and its model follows.

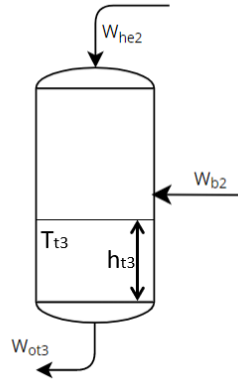


Figure 1.7: Tank 3 schematic

### Mass Balance

The mass balance is described by

$$\frac{dh_{t3}(t)}{dt} = \frac{1}{\rho \cdot A_{t3}} \cdot (w_{he2}(t) + w_{b2}(t) - w_{ot3}(t)) \quad (1.34)$$

with  $h_{t3}(t)$  the water level in the tank,  $A_{t3}$  the tank section,  $w_{he2}(t)$  the inlet mass flow from the secondary heat exchanger,  $w_{b2}(t)$  the inlet mass flow from the bypass 2 and  $w_{ot3}(t)$  the outlet mass flow.

Analysing the diagram and with the introduction of the bypass we obtain the conservation of the mass of the two tanks

$$w_{he2}(t) + w_{b2}(t) = w_{op2}(t) \quad (1.35)$$

Finally, replacing (1.35), we get

$$\frac{dh_{t3}(t)}{dt} = \frac{1}{\rho \cdot A_{t3}} \cdot (w_{op2}(t) - w_{ot3}(t)) \quad (1.36)$$

### Energy balance

The temperature dynamics inside Tank 3 is described by the following equation

$$\frac{dT_{t3}(t)}{dt} = \frac{1}{\rho \cdot A_{t3} \cdot h_{t3}(t)} \cdot (w_{b2}(t) \cdot T_{i2}(t) + w_{he2}(t) \cdot T_{heu}(t) - w_{op2}(t) \cdot T_{t3}(t)) - \beta_3 \cdot (T_{t3}(t) - T_{amb}(t)) \quad (1.37)$$

where  $T_{t2}(t)$ ,  $T_{t3}(t)$  and  $T_{heu}(t)$  are the temperature of the tank 2, of the tank 3 and the temperature of the mass flow coming from the secondary heat exchanger, respectively. Also in this case, is considered a loss by convention with the external environment and modelled by the coefficient  $\beta_3$ .

### Piping from Tank 3 to Tank 2

Between tank 3 and tank 2 there are no pumps to regulate the flow, but the water flow through the pipe through gravity force. Since the area of the short horizontal free discharge tube  $A_{out3}$  is much smaller than the tank area  $A_{t3}$ , the water speed into the tank is much smaller than the water speed  $u_{out3}(t)$  in the outlet pipe. By applying the momentum balance at the bottom and the outlet of the tank and assuming the pressure at the outlet to be equal to the atmospheric pressure, then it comes

$$P_{t3}(t) - P_{atm}(t) = \frac{1}{2} \rho \cdot u_{out3}(t)^2 \quad (1.38)$$

The mass flow is

$$w_{it2}(t) = \rho \cdot A_{out3} \cdot u_{out3}(t) \quad (1.39)$$

then, replace(1.39) in (1.38)

$$w_{it2}(t) = A_{out3} \cdot \sqrt{2\rho(P_{t3}(t) - P_{atm}(t))} \quad (1.40)$$

and apply Stevin's Law to the tank

$$P_{t3}(t) = P_{atm} + \rho \cdot g \cdot h_{t3}(t) \quad (1.41)$$

Finally, by substituting (1.41) in (1.40), we obtain

$$w_{it2}(t) = A_{out3} \cdot \rho \cdot \sqrt{2 \cdot g \cdot h_{t3}(t)} \quad (1.42)$$

So, in the end, the outlet mass flow from the tank 3 does not depend on the pressure drops, but only on the water level.

## Secondary heat exchanger

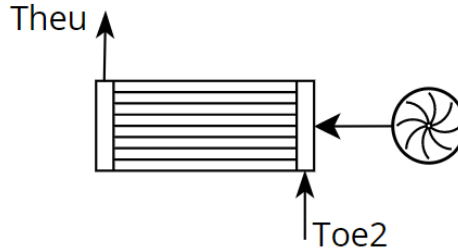


Figure 1.8: Secondary Heat Exchanger schematic

The secondary heat exchanger consists of a radiator into which the outlet water mass from the primary heat exchanger flows. Unlike the primary heat exchanger, there is only one water flow and thus the heat exchange takes place with the external environment. In addition, fans are mounted behind the exchanger so that there is the possibility of an additional cooling of the fluid. The control of these fans, that is, their switching on and off, is done manually by the operator.

Since the parameters of the fans and their model dynamics are not known, it is not possible to directly find the heat output extracted from the secondary heat exchanger and a model needs to be identified. The identification of this model is important for the purposes of this study because it allows the MPC control to predict the output temperature at the exchanger based on the optimized control actions. The identification of the secondary heat exchanger is possible thanks to the available sensors measuring the flow rate  $w_{he2}$  passing through the exchanger, the inlet and outlet temperatures,  $T_{oe2}$  and  $T_{heu}$ , and the ambient temperature  $T_{amb}$ .

### Black-Box Identification - ARX model

Identification was made using a black-box approach, which provides models in which the process is not viewed from the perspective of the physical laws, but rather it is known only through quantitative observations, experiments and measurements [10]. In principle, it is possible to build a black-box system without having any specific knowledge of the process to be modeled but only input/output data.

Among the possible model structures for identification, an ARX model in discrete-time domain was chosen. An ARX model is a polynomial model on the form:

$$y(k) = G(z) \cdot u(k) \quad (1.43)$$

where  $G$  is a rational transfer function in the  $z$ -translation operator that maps input values to output values:

$$G(z) = \frac{B(z)}{A(z)} = \frac{b_0 z^{-n_k} + b_1 z^{-n_k-1} + \dots + b_{n_b} z^{-n_k-n_b}}{1 + a_1 + \dots + a_{n_a} z^{-n_a}} \quad (1.44)$$

or explicitly:

$$\begin{aligned} y(k) + a_1 y(k-1) + \dots + a_{n_a} y(k-n_a) = \\ b_0 u(k-n_k) + b_1 u(k-n_k-1) + \dots + b_{n_b-1} u(k-n_k-n_b) \end{aligned} \quad (1.45)$$

Here, the numbers  $n_a$  and  $n_b$  are the orders of the respective polynomials. The number  $n_k$  is the number of delays from input to output. The eq.(1.45) refers to a SISO system, but the system under consideration is a MISO system. Infact, the objective is to identify a model that describes the trend of the outlet temperature from the exchanger,  $T_{heu}$ , the output, as a function of the input parameters, i.e., the flow rate  $w_{he2}$ , its temperature,  $T_{he2}$ , and the ambient temperature,  $T_{amb}$ . The general form for the case under consideration, so with one output and three inputs, is

$$y(k) = \sum_{i=1}^{n_a} a_i y(k-i) + \sum_{j=0}^{n_b-1} b_j u_1(k-j) + \sum_{j=0}^{n_b-1} b_j u_2(k-j) + \sum_{j=0}^{n_b-1} b_j u_3(k-j) \quad (1.46)$$

It's worth noting that the ARX model states are the past outputs and inputs, which are measurable. This enables to avoid the design of state observers. Identification was done using Matlab's "System identification toolbox". In particular, two different models are identified, one when the fans are off and one when the fans are on. The transition between one formulation and the other is handled by a variable  $\delta(t)$  which takes as its value either 0 or 1 depending on the state of the fans. The final models becomes:

$$y_1(k) = \sum_{i=1}^{n_a} a_i^1 y(k-i) + \sum_{j=0}^{n_b-1} b_{1j}^1 u_1(k-j) + \sum_{j=0}^{n_b-1} b_{2j}^1 u_2(k-j) + \sum_{j=0}^{n_b-1} b_{3j}^1 u_3(k-j) \quad (1.47a)$$

$$y_2(k) = \sum_{i=1}^{n_a} a_i^2 y(k-i) + \sum_{j=0}^{n_b-1} b_{1j}^2 u_1(k-j) + \sum_{j=0}^{n_b-1} b_{2j}^2 u_2(k-j) + \sum_{j=0}^{n_b-1} b_{3j}^2 u_3(k-j) \quad (1.47b)$$

$$y(k) = \delta(k) y_1(k) + (1 - \delta(k)) y_2(k) \quad (1.48)$$

where  $y(k) = T_{heu}(k)$  and  $u(k) = [T_{amb}(k), T_{he2}(k), w_{he2}(k)]'$ .

## 1.4. Final Formulation

This section summarizes the equations derived in the previous paragraphs that are useful for representing the behavior of the system and for its control.

### Primary Circuit

#### Tank 1

$$\dot{T}_{t1}(t) = \frac{P_e(t)}{m \cdot c_w} + \frac{w_{he1}(t)}{m} \cdot (T_{oe1}(t) - T_{t1}(t)) \quad (1.49)$$

#### Primary Heat Exchanger

$$\dot{Q}_{12}(t) = \epsilon \cdot \dot{Q}_{max}(t) = \epsilon \cdot c_w \cdot \min(w_{he1}, w_{he2}) \cdot (T_{t1}(t) - T_{t2}(t)) \quad (1.50)$$

$$T_{oe1}(t) = T_{t1}(t) - \frac{\dot{Q}_{12}(t)}{c_w \cdot w_{he1}(t)} \quad (1.51)$$

$$T_{oe2}(t) = T_{t2}(t) + \frac{\dot{Q}_{12}(t)}{c_w \cdot w_{he2}(t)} \quad (1.52)$$

### Secondary Circuit

#### Tank 2

$$\dot{T}_{t2}(t) = \frac{w_{it2}(t)}{\rho \cdot A_{t2} \cdot h_{t2}(t)} \cdot (T_{t3}(t) - T_{t2}(t) - \beta_2 \cdot (T_{t2}(t) - T_{amb}(t))) \quad (1.53)$$

#### Level Tank 2

$$\dot{h}_{t2}(t) = \frac{1}{\rho \cdot A_{t2}} \cdot (w_{it2}(t) - w_{op2}(t)) \quad (1.54)$$

### Tank 3

$$\begin{aligned} \dot{T}_{t3}(t) = & \\ \frac{1}{\rho \cdot A_{t3} \cdot h_{t3}(t)} \cdot & (w_{b3}(t) \cdot T_{t2}(t) + w_{he2}(t) \cdot T_{heu}(t) - w_{op2}(t) \cdot T_{t3}(t)) - \beta_3 \cdot (T_{t3}(t) - T_{amb}(t)) \end{aligned} \quad (1.55)$$

### Level Tank 3

$$\dot{h}_{t3}(t) = \frac{1}{\rho \cdot A_{t3}} \cdot (w_{op2}(t) - w_{ot3}(t)) \quad (1.56)$$

### Piping from Tank 3 to Tank 2

$$w_{it2}(t) = A_{out3} \cdot \rho \cdot \sqrt{2 \cdot g \cdot h_{t3}(t)} \quad (1.57)$$

### Secondary Heat Exchanger (Discrete Time)

$$y_1(k) = \sum_{i=1}^{n_a} a_i^1 y(k-i) + \sum_{j=0}^{n_b-1} b_{1j}^1 u_1(k-j) + \sum_{j=0}^{n_b-1} b_{2j}^1 u_2(k-j) + \sum_{j=0}^{n_b-1} b_{3j}^1 u_3(k-j) \quad (1.58a)$$

$$y_2(k) = \sum_{i=1}^{n_a} a_i^2 y(k-i) + \sum_{j=0}^{n_b-1} b_{1j}^2 u_1(k-j) + \sum_{j=0}^{n_b-1} b_{2j}^2 u_2(k-j) + \sum_{j=0}^{n_b-1} b_{3j}^2 u_3(k-j) \quad (1.58b)$$

$$y(k) = \delta(k)y_1(k) + (1 - \delta(k))y_2(k) \quad (1.59)$$

where  $y(k) = T_{heu}(k)$  and  $u(k) = [T_{amb}(k), T_{he2}(k), w_{he2}(k)]'$ .



## 1.5. Summary

After defining the fundamental equations, it is appropriate to define the control and controlled variables. The chosen control variables are:

- $P_e(t)$ , the power supplied by the heater to warm the water in Tank 1.
- $w_{he1}(t)$ , the mass flow rate circulating into the primary heat exchanger, primary-side, which can be directly imposed thanks to a local PID regulator acting on valve 1 and 2 (see Figure 1.2)
- $w_{he2}(t)$ , the mass flow rate circulating into the primary heat exchanger, secondary-side, which can be directly imposed thanks to a local PID regulator acting on valve 3 and 4 (see Figure 1.3)

As already explained, the desired flow rate values are directly imposed, and the PLC will then calculate the value of the bypass flow rates and manage the opening of the valves. The controlled variables are:

- $T_{t1}(t)$ , the temperature of the Tank 1, that is also the primary circuit water temperature entering into the primary heat exchanger.
- $T_{t2}(t)$ , the temperature of the Tank 2, that is also the secondary circuit water temperature entering into the primary heat exchanger.
- $T_{t3}(t)$ , the temperature of the Tank 3.



## 2 | Simulator development and validation

Starting from the equations described in the previous chapter and summarized in Section 1.4, a Simulink model of the system was developed. The simulation model has three main blocks, *Primary Circuit*, *Secondary Circuit* and *Secondary Heat Exchanger*. In each of these blocks, the models of the various components previously described are implemented. This simulation blocks are explained in detail in the following.

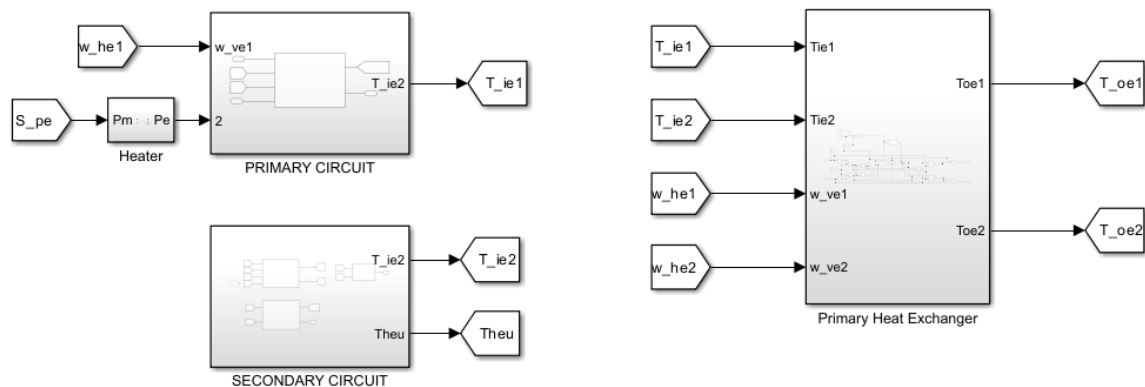


Figure 2.1: Simulink model of the plant

## 2.1. Primary Circuit simulation model

### 2.1.1. Tank 1

The primary circuit block models the dynamics of the temperature of tank 1. Recalling the equation derived earlier in section (1.3.1) one obtains from the energy balance:

$$\dot{T}_{t1}(t) = \frac{P_e(t)}{m \cdot c_w} + \frac{W_{he1}(t)}{m} \cdot (T_{oe1}(t) - T_{t1}(t)) \quad (2.1)$$

This formula is implemented in Simulink, eventually integrating  $\dot{T}_{t1}$  to obtain  $T_{t1}$ . Its implementation is shown in Figure 2.2.

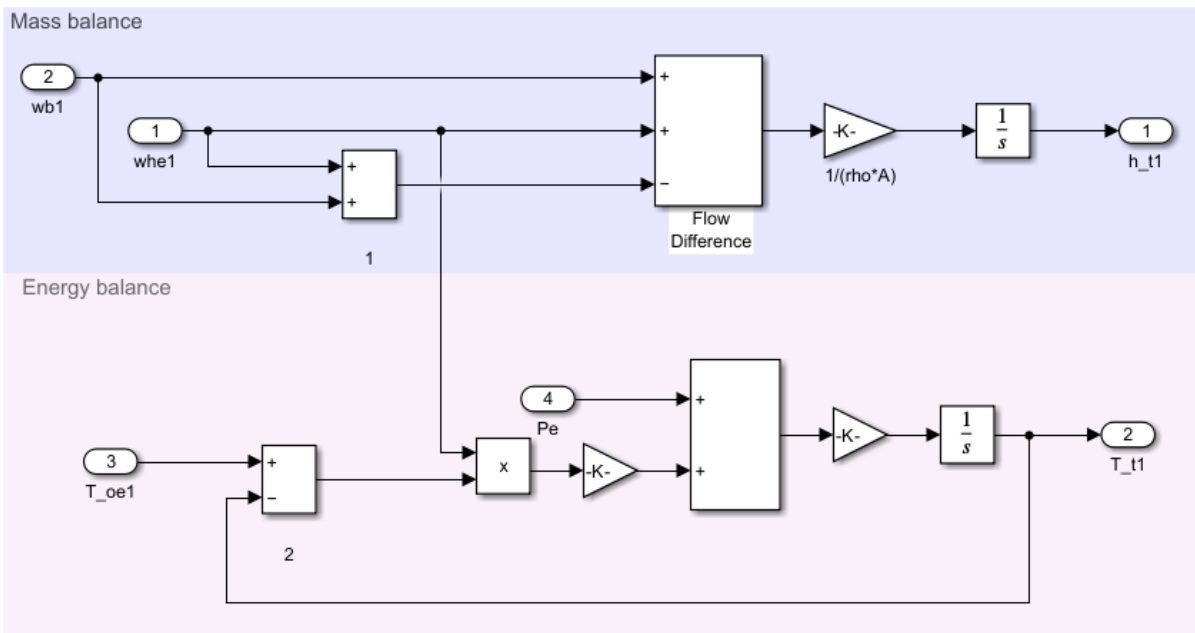


Figure 2.2: Tank 1 simulation model

The mass balance, eq. (1.12), is also modeled in Figure 2.2, even though the change in water mass level remains constant since the mass entering the reservoir is equal to the mass leaving it.

### 2.1.2. Heater

The heater block models the power supplied to the thermal resistor of tank 1. As already explained the power cannot be continuously modulated, but it can only deliver either 0 W or the maximum value, 2200 W. To do this, the PLC uses PWM modulation and manages



where  $w_{he1}$  and  $w_{he2}$  are the values of the flow rates passing through the exchanger, primary and secondary sides, respectively,  $T_{t1}$  and  $T_{t2}$  the inlet temperatures of the latter,  $c_w$  the specific heat of water,  $\dot{Q}_{12}$  the heat power exchanged by the two circuits. Since the only unknown is the power exchanged, the implemented block performs its own calculation, while the other quantities mentioned are its inputs. The  $\epsilon$ -NTU method, explained in Section 1.3.2, is used for its calculation. The simulink block is shown in Figure 2.4.

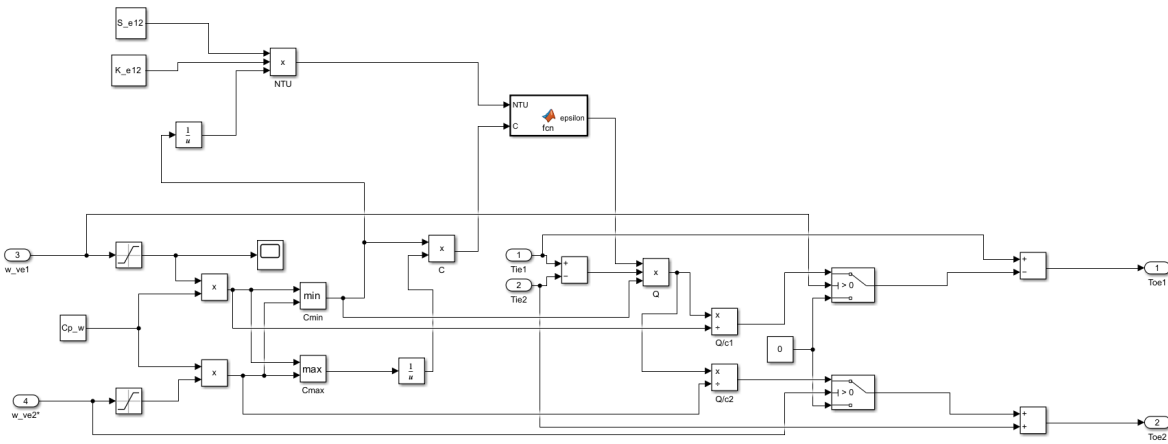


Figure 2.4: Primary Heat Exchanger with NTU method simulation model

### 2.3. Secondary Circuit simulation model

In the secondary circuit block, there are two tanks blocks, Tank 2 and Tank 3, and the secondary heat exchanger block as depicted in Figure 2.5.

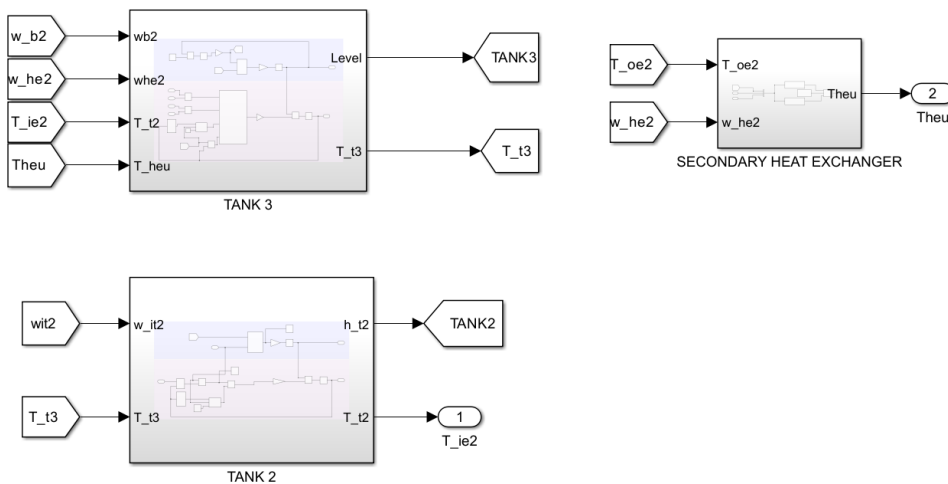


Figure 2.5: Secondary Circuit simulation model

The modeling of the two tanks is similar to what has already been seen for Tank 1, but unlike the primary these do not have the thermal resistor inside them, and in addition the variation of the two levels must be considered. This is because, as already seen, water height in this tanks is not constant. In the next sections, the various blocks are presented in detail.

### 2.3.1. Tank 2

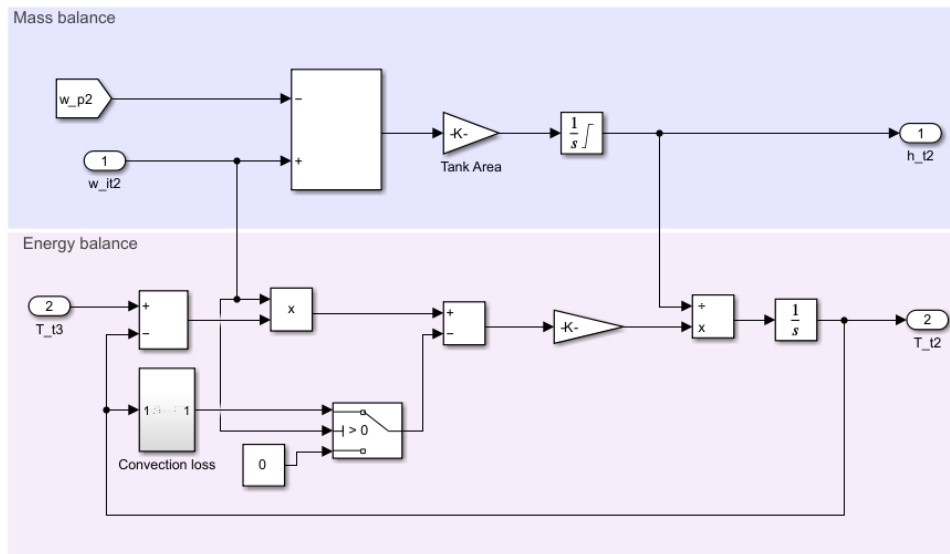


Figure 2.6: Tank 2 simulation model

Tank 2 has an inlet flow rate,  $w_{it2}$ , which is also the outlet flow rate of Tank 3, which due to the geodesic height difference between the two tanks flows into the pipe connecting them. The outlet flow rate,  $w_{op2}$  corresponds to the pump 2 flow rate.

As already seen in the modeling of Tank 1, the equation implemented in Simulink is the integration of the temperature variation obtained from the energy balance of Tank 2.

### 2.3.2. Tank 3 simulation model

The Tank 3 has two inlets and one output. As in Tank 2, the water level must be considered as it is a varying parameter in the energy balance equation.

It is important to notice that the sum of the two incoming flow rates, i.e., the flow rate from the secondary exchanger,  $w_{he2}$ , and the flow rate from bypass 2,  $w_{b2}$ , is nothing more than the flow rate of pump 2,  $w_{op2}$ . That is why in the final equation, (1.56), this sum has already been substituted and it is the equation that has been implemented in Simulink.

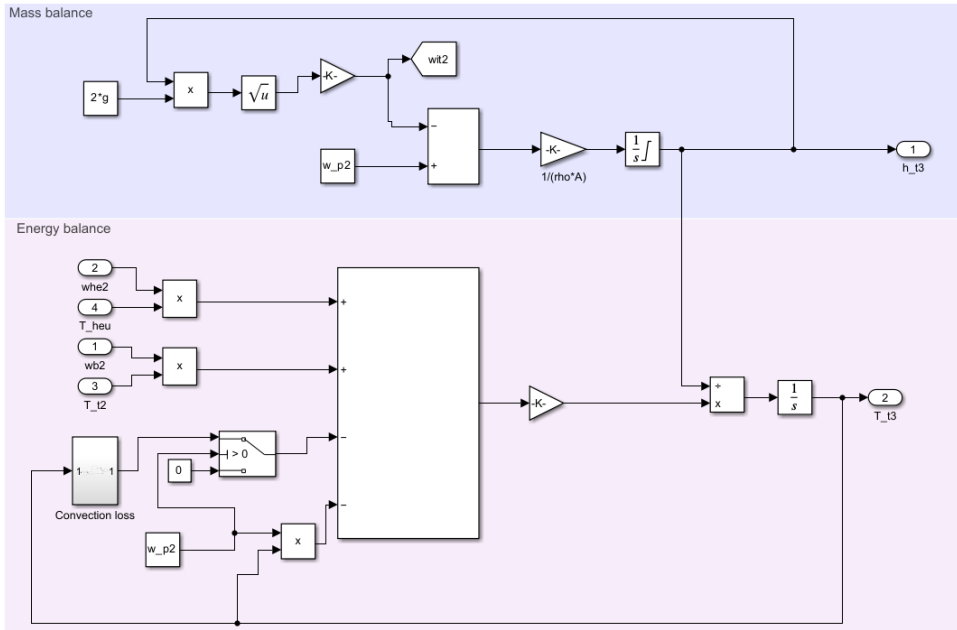


Figure 2.7: Tank 3 simulation model

The calculation of the value of the output flow rate,  $w_{ot3}$ , on the other hand, was implemented, as explained in section (1.3.3), with the formula:

$$w_{it2}(t) = A_{out3} \cdot \rho \cdot \sqrt{2 \cdot g \cdot h_{t3}(t)} \quad (2.6)$$

### 2.3.3. Secondary Heat Exchanger

The last component that is discussed is the secondary heat exchanger. The model of this element was identified by black-box identification, resulting as an ARX model. As explained in Section 1.3.3, two ARX models have been identified, one when the fans are not active and one when they are active. Switching between models is managed by a switch block. The selection criterion is handled by a 0 or 1 fan signal according to the state of the fans, remember that their activation is done manually by a user. To be able to implement the two ARX models and thus be able to simulate them, their state-space representation must be found. This is described in the next subsection discusses the procedure, among possible ones, used to find it.



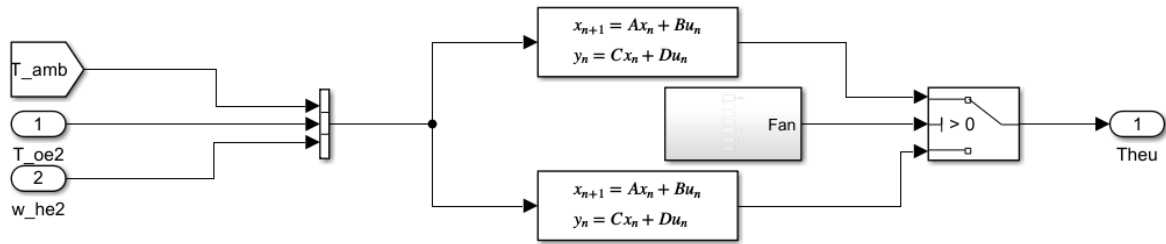


Figure 2.8: Secondary Heat Exchanger simulation model

## ARX models identification and state-space representation

Recalling the discrete-time polynomial representation of an ARX model:

$$y(k) = \sum_{i=1}^{na} a_i y(k-i) + \sum_{j=0}^{nb-1} b_j u(k-j) \quad (2.7)$$

The discrete-time state-space representation is:

$$\begin{cases} x(k+1) = Ax(k) + Bu(k) \\ y(k) = Cx(k) + Du(k) \end{cases} \quad (2.8)$$

the first step is to define the states as

$$x(k) = \begin{bmatrix} y(k-1) \\ y(k-2) \\ \vdots \\ y(k-n_a) \\ u(k-1) \\ u(k-2) \\ \vdots \\ u(k-n_b) \end{bmatrix} \quad x(k+1) = \begin{bmatrix} y(k) \\ y(k-1) \\ \vdots \\ y(k-n_a+1) \\ u(k) \\ u(k-1) \\ \vdots \\ u(k-n_b+1) \end{bmatrix} \quad (2.9)$$

Then, the next step is to derive the matrices for the system:

$$\begin{aligned}
 \mathbf{A} &= \begin{bmatrix} -a_1 & \dots & \dots & \dots & -a_{n_a} & b_1 & \dots & \dots & \dots & b_{n_b-1} \\ & & I_{(n_a-1),(n_a-1)} & & 0 & & & O_{(n_a-1),(n_b-2)} & & 0 \\ 0 & \dots & \dots & \dots & 0 & 0 & \dots & \dots & \dots & 0 \\ & & O_{(n_b-1),(n_a-1)} & & 0 & & & I_{(n_a-1),(n_b-2)} & & 0 \end{bmatrix} \\
 \mathbf{B} &= \begin{bmatrix} b_0 \\ 0 \\ \cdot \\ \cdot \\ 0 \\ 1 \\ 0 \\ \cdot \\ \cdot \\ 0 \end{bmatrix} \quad \mathbf{C} = \begin{bmatrix} -a_1 & \cdot & \cdot & \cdot & -a_{n_a} & b_1 & \cdot & \cdot & \cdot & b_{n_b-1} \end{bmatrix} \quad \mathbf{D} = b_0
 \end{aligned} \tag{2.10}$$

Where  $\mathbf{A}$  is a  $(n_a + n_b - 1) \times (n_a + n_b - 1)$  matrix,  $\mathbf{B}$  is  $(n_a + n_b - 1) \times 1$ ,  $\mathbf{C}$   $p \times (n_a + n_b - 1)$  and  $\mathbf{D}$   $p \times 1$ . Where  $m$  is the number of inputs and  $p$  the number of outputs.

## Identification Procedure

The aim of the identification procedure is to identify the parameters of the two previously introduced ARX models, i.e., one with and one without fan activation; for this purpose, several experiments were carried out under the two conditions in order to have a complete data set.

The identification process was performed by estimating parameters using the System Identification toolbox in MATLAB. This toolbox solves an overdetermined set of linear equations representing a least-squares estimation problem.

Defining

$$\theta = \begin{bmatrix} a_1 \\ \vdots \\ a_{n_a} \\ b_0 \\ \vdots \\ b_{n_b} \end{bmatrix} \quad \psi(k) = \begin{bmatrix} y(k-1) \\ y(k-2) \\ \vdots \\ y(k-n_a) \\ u(k-1) \\ u(k-2) \\ \vdots \\ u(k-n_b-1) \end{bmatrix} \quad (2.11)$$

the least-squares criterion aims to compute the value of  $\theta$  that minimizes the quantity [4]

$$J(\theta) = \frac{1}{N} \cdot \sum_{i=1}^N (y(i) - \theta^T \cdot \psi(i))^2 \quad (2.12)$$

where  $y(i)$  are the measurable outputs values and eq. (2.12) represents the mean square error between measured and predicted values. Since these values were acquired with a period of 20 seconds during the experiments, it was also chosen to use this value as the sampling time for the model identification procedure. The orders of the model have been selected by evaluating the model performance over the validation dataset and selected the one with the best fits.

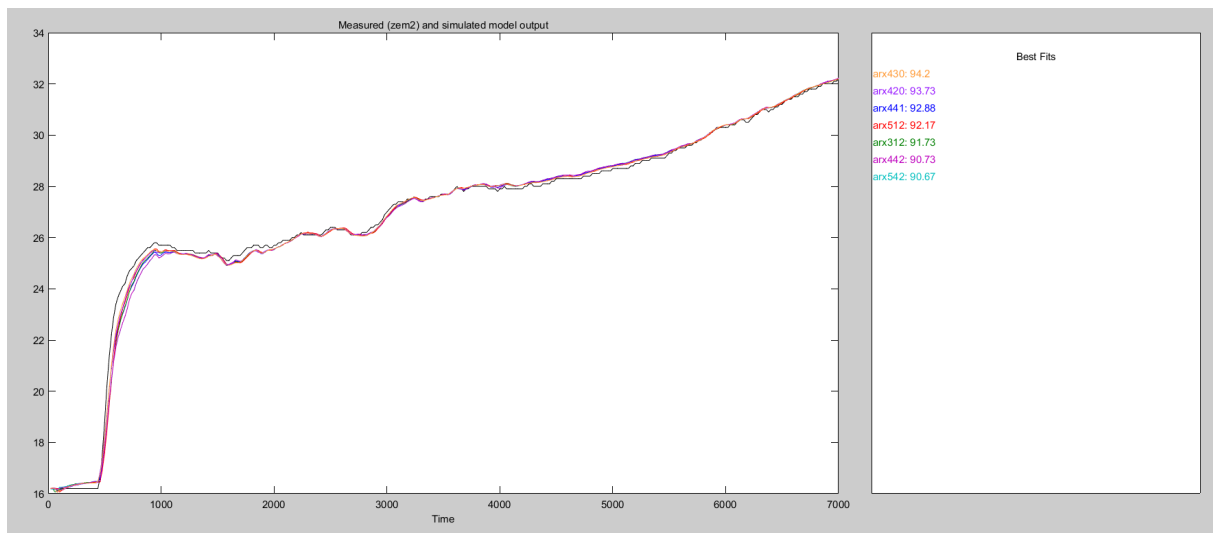


Figure 2.9: Comparison of performances among ARX models with different orders in validation

It can be clearly seen from the Figure 2.9 that the model with the best fits is the one with

the orders of the polynomials, i.e.  $n_a$  and  $n_b$ , equal to 4 and 3, respectively.

At this stage, the identification has been performed. The selected inputs/outputs are

- $m = 3$ , the three inputs are the ambient temperature,  $T_{amb}$ , the mass flow rate from the primary heat exchanger  $W_{he2}$ , and its temperature,  $T_{oe2}$ ;
- $p = 1$ , the only output is the temperature of the mass flow rate leaving the secondary heat exchanger and entering the Tank 3,  $T_{heu}$ .

And the selected model orders are the following

- $n_a = 4$ ;
- $n_b = 3$ ;

So, the structure of the be identified is:

$$\mathbf{A} = \begin{bmatrix} -a1 & -a2 & -a3 & -a4 & b_1^1 & b_2^1 & b_1^2 & b_2^2 & b_1^3 & b_2^3 \\ 1 & 0 & 0 & 0 & 0 & 0 & 0 & 0 & 0 & 0 \\ 0 & 1 & 0 & 0 & 0 & 0 & 0 & 0 & 0 & 0 \\ 0 & 0 & 1 & 0 & 0 & 0 & 0 & 0 & 0 & 0 \\ 0 & 0 & 0 & 0 & 0 & 0 & 0 & 0 & 0 & 0 \\ 0 & 0 & 0 & 0 & 1 & 0 & 0 & 0 & 0 & 0 \\ 0 & 0 & 0 & 0 & 0 & 0 & 0 & 0 & 0 & 0 \\ 0 & 0 & 0 & 0 & 0 & 0 & 1 & 0 & 0 & 0 \\ 0 & 0 & 0 & 0 & 0 & 0 & 0 & 0 & 0 & 0 \\ 0 & 0 & 0 & 0 & 0 & 0 & 0 & 0 & 1 & 0 \end{bmatrix} \quad \mathbf{B} = \begin{bmatrix} b_0^1 & b_0^2 & b_0^3 \\ 0 & 0 & 0 \\ 0 & 0 & 0 \\ 0 & 0 & 0 \\ 1 & 0 & 0 \\ 0 & 0 & 0 \\ 0 & 1 & 0 \\ 0 & 0 & 0 \\ 0 & 0 & 1 \\ 0 & 0 & 0 \end{bmatrix} \quad (2.13)$$

$$\mathbf{C} = \begin{bmatrix} -a1 & -a2 & -a3 & -a4 & b_1^1 & b_2^1 & b_1^2 & b_2^2 & b_1^3 & b_2^3 \end{bmatrix} \quad \mathbf{D} = \begin{bmatrix} b_0^1 & b_0^2 & b_0^3 \end{bmatrix} \quad (2.14)$$

## 2.4. Simulation Model Validation

Validation of the overall model is useful in order to verify that the simplifications introduced and their related implementations in the software are correct. To do this, therefore, experiments have been carried out on the actual plant in order to have the useful measurements available. As already noted, the aim is to focus on the thermal dynamics, and thus on the temperature trends of the three tanks. So to check the validity of the model, the acquisitions of these quantities,  $T_{t1}$ ,  $T_{t2}$  and  $T_{t3}$ , were compared with the simulated quantities,  $T_{t1sim}$ ,  $T_{t2sim}$  and  $T_{t3sim}$ . During the tests, the flow rate values provided to the simulator are the actual values provided by the respective flow sensors during the

experiments. The first experiment performed concerns a test without fan activation and without modelling the heat losses through the ambient, i.e.  $\beta_2 = \beta_3 = 0$ . The results are illustrated in the following figure.

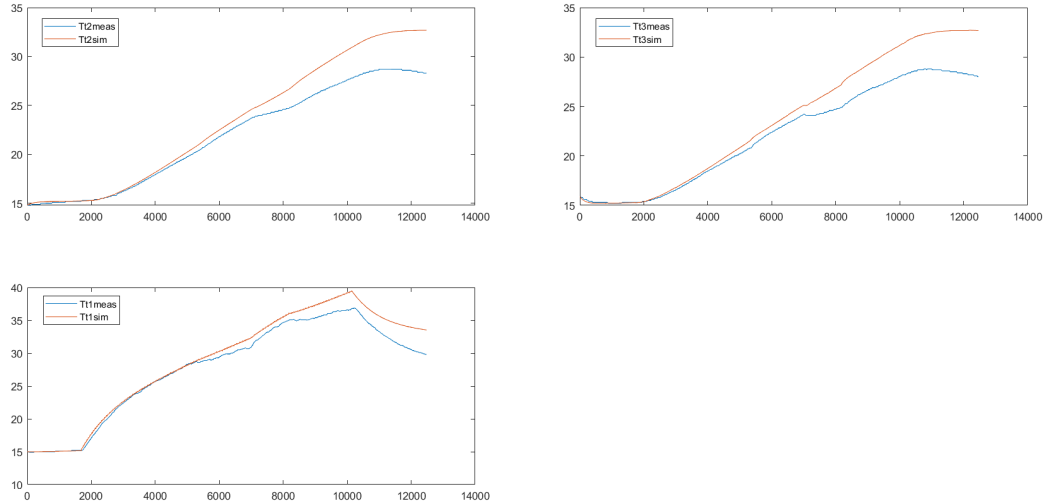


Figure 2.10: Comparison of the three measured temperatures (in blue) with simulated temperatures (in red). In this experiment, the fans are not active.

As mentioned above and as can be seen from the graphs in Figure 2.10, it was immediately apparent that without the contribution due to convection losses with the environment in the equations of temperature variation, the simulated model overestimates these quantities. Through these experiments, the heat loss parameters are estimated, i.e.  $\beta_2 = 0.012$  and  $\beta_3 = 0.059$ . Once these parameters were introduced into the model as extensively discussed in the previous paragraphs, a new experiment was performed to verify and validate them, obtaining the results in Figure 2.11.

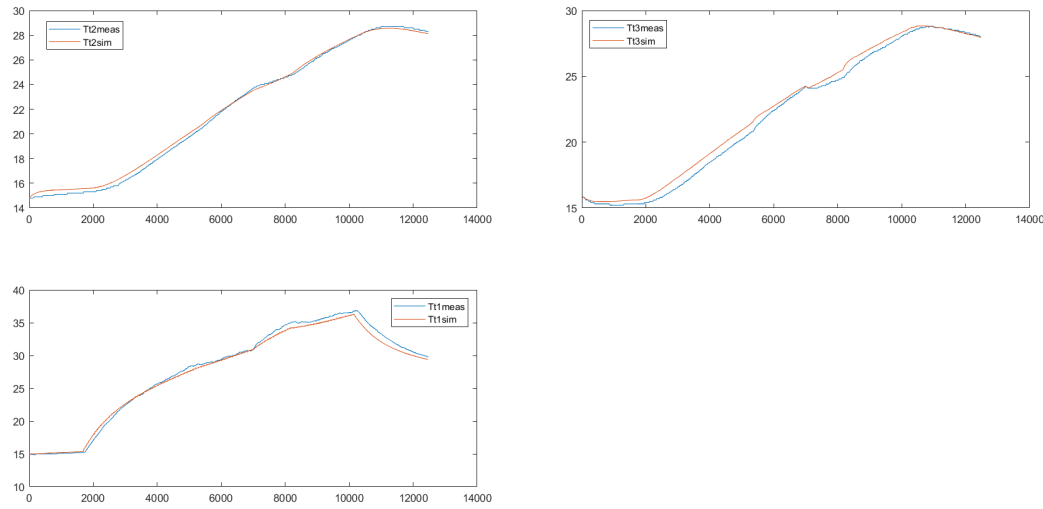


Figure 2.11: The same test as before but this time with the contribution that considers the convection losses with the environment.

As already mentioned, this experiment was very useful because it allowed to complete the identification of heat losses with the environment in Tanks 2 and 3. Hence, after the two balance equations were modified, that graph was obtained in which the simulator follow the actual values very well. To complete the validation, further tests were performed with fan activation. Two of these experiments are shown in the following. Specifically, in the experiment in Figure 2.13, other tests were performed such as closing valve 1, which is the valve that controls the flow circulating to the primary heat exchanger in the primary circuit. In this way, water circulates only in the bypass circuit and as it can be seen, the temperature of Tank 1 has a quite considerable increment. Therefore, with this experiment it was also useful to calculate the actual power delivered by the electrical resistors in the tank.

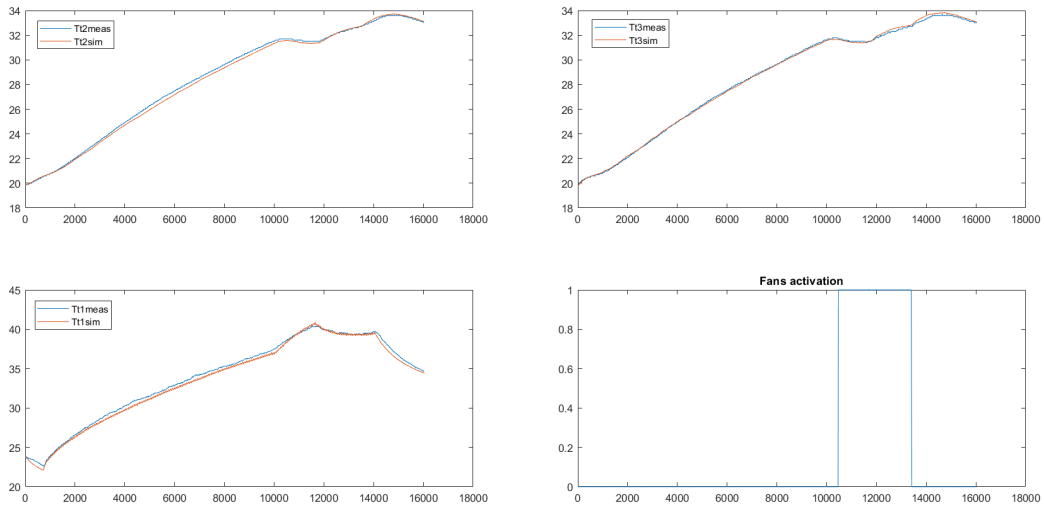


Figure 2.12: In addition to the graphs comparing measured and simulated temperatures, the bottom right graph shows the timing of fan on and off (1 means on and 0 off).

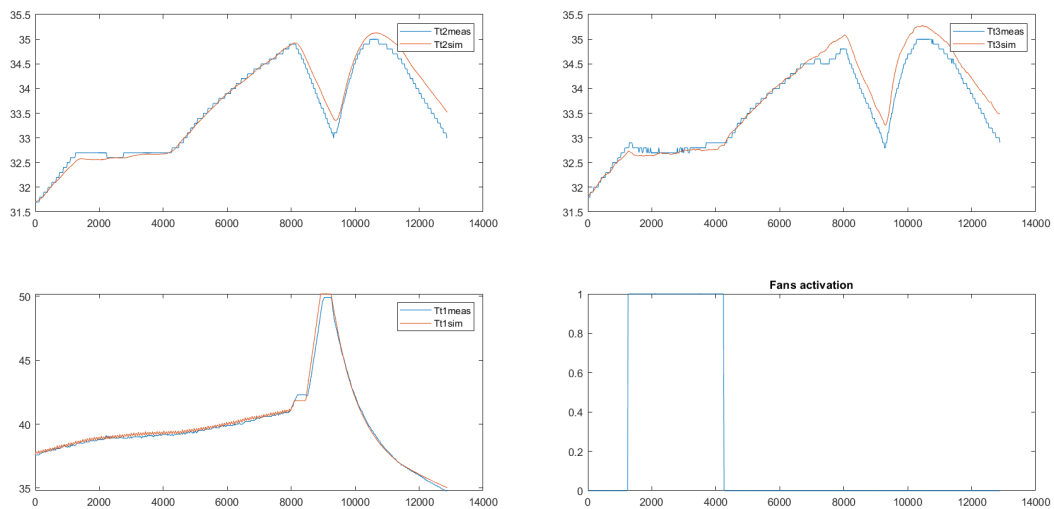


Figure 2.13: Further test with fan activation. In this test, the influence of the fans on the trend of  $T_2$  and  $T_3$  in the early part of the experiment is significantly noticeable.

The results obtained are very satisfactory and confirm the assumptions and choices made in modeling the plant. A mathematical formulation that well describes the process and a validated model of it are the basis for being able to start designing a control system.





# 3 | MPC Design and simulation

This chapter describes the choice and implementation of the control law tested, for now, on the Simulink model. This is due to the possibility of having a model of the entire plant that is very faithful to reality, as shown with the results obtained and described in the previous chapter. The control is based on the use of Model Predictive Control (MPC) approach. This is a widely used technique with many advantages that is discussed in the following sections. Results obtained with a classical implementation of the control algorithm are initially discussed, and then a strategy called the "*input blocking strategy*" is discussed.

## 3.1. MPC

Model predictive control (MPC) is one of the most successful and most popular advanced control methods. It was first introduced in the 1970s for the process and chemical industries and has been the subject of academic studies and growing industrial interest since then.

The term MPC identifies a large family of algorithms that make explicit use of the model used to describe the process, usually in discrete-time domain. The main objective is to obtain the optimal control signal for the minimization of a certain cost function that reflects the performance of the system. The main feature therefore that distinguishes it from standard control techniques is that the control problem is formulated as an optimization one.

It makes use of the so-called "Receding Horizon" (RH) principle in which at each sampling time an FHOCP (Finite Horizon Optimal Control Problem) is solved, initializing the model at the current, measured state value. Specifically, at each time instant an optimal control law is defined over some predefined time horizon; e.g. starting from the current instant  $k$  up to  $k + N$ . The cost function  $J$  is minimized with respect to the control law sequence, the first optimal control input is then applied to the system and then repeated such calculation in the next interval  $[k + 1, k + 1 + N]$  [11].

By applying the control input of the first step and not the entire optimal sequence, a

closed-loop control law is obtained. In Figure 3.1 is represented a graphical representation of the basic idea of RH principle.

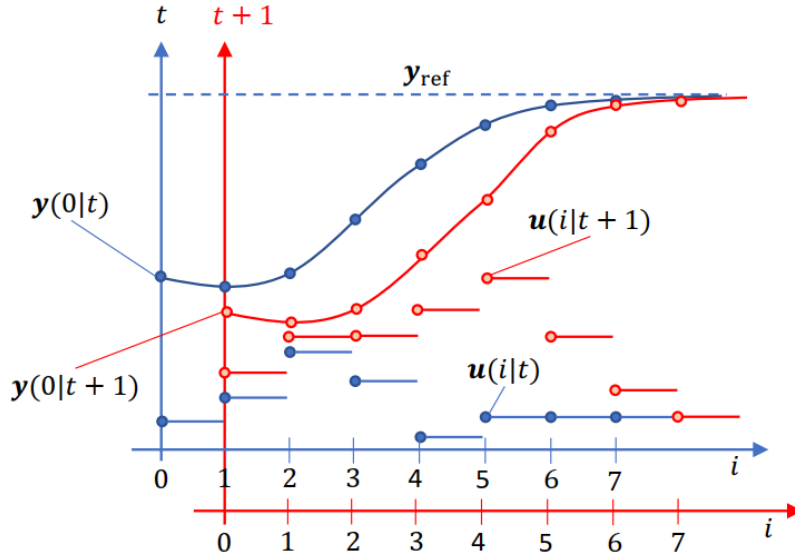


Figure 3.1: Graphic representation of Receding Horizon principle [5].

The main advantages of MPC are: the ability to design control systems for large multiple input and multiple output (MIMO) systems, the ability to introduce input, output, and state constraints, and the possibilities to deal with nonlinear systems. The main disadvantage lies in the fact that the MPC performs an optimization at each sampling time and thus it may require a large amount of real-time computation [15]. In fact, early uses were mainly for low sample frequency systems, but the recent advances in computing hardware and software have also greatly reduced the cost and improved the speed and reliability of these computations expanding the fields of use of these algorithms.

## 3.2. Nonlinear MPC

When dealing with nonlinear systems normally a common strategy is to use a linearized model of the system. But since the system under investigation does not have large nonlinearities, it was decided to use a Nonlinear Model Predictive Control (NMPC) formulation [1]. It is considered a generic nonlinear discrete-time system in the form:

$$x(k+1) = f(x(k), u(k), d(k)) \quad (3.1)$$

Where  $f(x, u, d)$  is a continuously differentiable function,  $x \in \mathfrak{R}^{n_x}$  the vector representing the state and  $u \in \mathfrak{R}^{n_u}$  the input vector and  $d$  the disturbances. The next step is to solve at each sample time  $k$  a FHOCP, that consist in found the optimal control sequence  $U(k) = [u(k), u(k+1), \dots, u(k+N-1)]$  that minimize a cost function:

$$J(x(k), U(k), D(k)) = \sum_{i=0}^{N-1} l(x(k+i), u(k+i)) \quad (3.2)$$

with  $l(., .)$  a suitable function in the state and output,  $N \in \mathbb{Z}^+$  the prediction horizon. As mentioned earlier, one of the advantages of MPC is the possibility of introducing constraints on inputs, outputs and states, such as:

$$\begin{aligned} u_{min} &\leq u(k+i) \leq u_{max} & i = 0, \dots, N-1 \\ y_{min} &\leq y(k+i) \leq y_{max} & i = 1, \dots, N \\ x_{min} &\leq x(k+i) \leq x_{max} & i = 1, \dots, N \end{aligned} \quad (3.3)$$

In this way, future values of the optimization variables are constrained not to exceed appropriate minimum and maximum values. To summarize, then at each time instant  $k$  an optimization problem is solved in the following formulation:

$$\begin{aligned} \min_U & J(x(k), U(k)) \\ \text{s.t.} & x(i+1|k) = f(x(i|k), u(i|k)), \quad i = 0, \dots, N-1, \\ & g(x(i|k), u(i|k)) = 0, \quad i = 0, \dots, N, \\ & h(x(i|k), u(i|k)) \geq 0, \quad i = 0, \dots, N, \\ & h_{final}(x(N|k), u(N|k)) \geq 0, \\ & x(0|k) = x_0 \end{aligned} \quad (3.4)$$

Where  $g$  and  $h$  represent the state and input constraints functions, the last two constraints represent respectively the terminal constraint and the initial condition, usually  $x_0$  is the vector containing the actual measured values. Then, according to the Receding Horizon principle, only the first element of the optimal control sequence  $U(k) = [u(0|k), \dots, u(N-1|k)]$  is applied to the system, i.e.  $u(0|k)$ , and then at the next time instant  $k+i$  the procedure is repeated.

### 3.2.1. NMPC formulation for tracking reference

The chosen cost function to be minimized to find the optimal sequence in this particular case is the following [6]:

$$J(x(k), U(k)) = \sum_{i=0}^{N-1} (\|x(i+1|k) - x^{ref}\|_Q^2 + \|\Delta u(i+1|k)\|_R^2) \quad (3.5)$$

Where  $Q = Q' \geq 0$  and  $R = R' > 0$  are matrices of suitable dimension. The cost function is composed of two terms, the first consists of the weighted quadratic error between the value of the predicted controlled variable and the reference one.

The second term is the weighted quadratic error between two successive optimal input sequences, which is defined as:

$$\Delta u(k+1) = u(k+1) - u(k) \quad (3.6)$$

The inputs considered and thus the control variables selected are three: the power supplied by the electrical resistance present in Tank 1,  $P_e$ , and the two flow rates passing through the primary heat exchanger,  $w_{he1}$  and  $w_{he2}$ , primary and secondary sides, respectively.

Constraints on the future values of states, inputs, and input variations are also introduced:

$$\begin{aligned} X_{min} &\leq X(k) \leq X_{max} \\ U_{min} &\leq U(k) \leq U_{max} \\ \delta U_{min} &\leq \Delta U(k) \leq \delta U_{max} \end{aligned} \quad (3.7)$$

The constraints on the inputs and their variations are implemented as hard constraints, in fact they can always be satisfied because the control variables are the result of the optimization procedure, so our choices. Instead, the states constraints can not be always satisfied, for example in presence of disturbances, so they are introduced as soft constraints

by means of slack variables. The new NMPC formulation becomes:

$$\begin{aligned}
 \min_{\Delta u} \quad & \sum_{i=0}^{N-1} (\|x(i+1|k) - x^{ref}\|_Q^2 + \|\Delta u(i+1|k)\|_R^2) + \rho s \\
 \text{s.t.} \quad & x(i+1|k) = f(x(i|k), u(i|k)), \quad i = 0, \dots, N-1, \\
 & x(0|k) = x_0, \\
 & U_{min} \leq U(k) \leq U_{max}, \\
 & \delta U_{min} \leq \Delta U(k) \leq \delta U_{max}, \\
 & X_{min} - sI \leq X(k) \leq X_{max} + sI, \\
 & s \geq 0
 \end{aligned} \tag{3.8}$$

where  $s$  is a vector of slack variables and  $x_0$  the measured state.

### 3.3. Case study: Implementation and Simulation

Thus, the goal of the NMPC algorithm introduced in the previous paragraph is to track the given Tank temperature references by minimizing the error between the predicted output and the reference. It was chosen to give the temperature values of Tank 1 and Tank 2 as references. The exclusion of the temperature of Tank 3 as a reference is due to the fact that, remembering the structure of the plant, Tank 2 and 3 are connected simply by a pipe and water flows by gravity, consequently the temperatures are related. The control scheme is implemented in Simulink is illustrated in Figure 3.2:

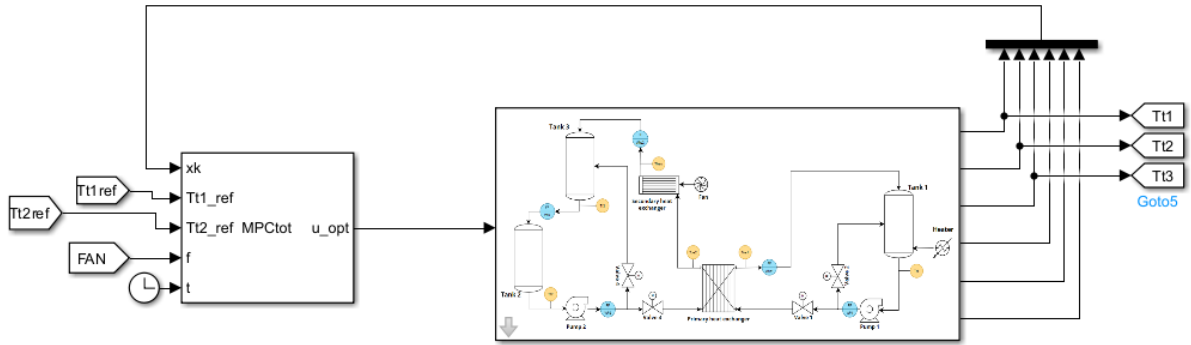


Figure 3.2: Simulink model used for MPC control. On the right we have the Simulink model of the plant and on the left a Matlab.System block in which the optimization is performed.

The NMPC was chosen to be implemented using CasADI and IPOPT as solvers within Matlab. CasADI is an open-source software tool for numerical optimization in general and optimal control (i.e. optimization involving differential equations) in particular. IPOPT or 'Interior Point Optimizer' is a large-scale nonlinear programming (NLP) solver that implements an interior point line search filter method that aims to find a local solution of a nonlinear problem [2].

### 3.3.1. Predictive Model of the Plant

Recalling the mathematical formulation of an optimization problem (3.4), one of the main ingredients of the MPC is a model describing the behavior of the dynamic system to be controlled to be included as a constraint. The function of this model is to predict the trends of the state variables starting from an initial state  $x_0$  for a prediction horizon  $N$ . The states, control variables and disturbances of our system are:

$$X(t) = \begin{bmatrix} h_{t2}(t) \\ h_{t3}(t) \\ T_{t1}(t) \\ T_{t2}(t) \\ T_{t3}(t) \end{bmatrix} \quad U(t) = \begin{bmatrix} P_e(t) \\ w_{he1}(t) \\ w_{he2}(t) \end{bmatrix} \quad D(t) = T_{amb}(t) \quad (3.9)$$

The equations used and describing the process are well known, and their derivation is discussed extensively in the previous chapter. As for the primary heat exchanger, it was necessary to simplify its model. Since CasADI has difficulty in dealing with Boolean-type variables, the  $\epsilon - NTU$  model cannot be used. The solution found was to rely on the following formula for calculating the power exchanged:

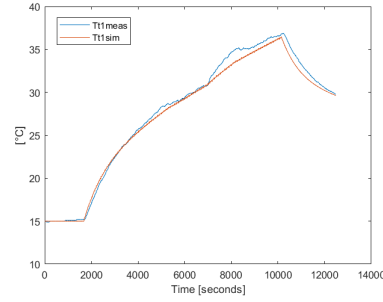
$$Q_{12}(t) = K_{12} \cdot A_{12} \cdot \frac{\Delta T_1(t) + \Delta T_2(t)}{2} \quad (3.10)$$

where:

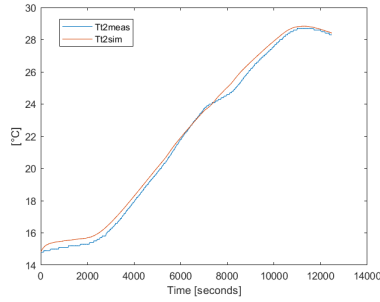
$$\begin{aligned} \Delta T_1(t) &= T_{t1}(t) - T_{oe2}(t) \\ \Delta T_2(t) &= T_{oe1}(t) - T_{t2}(t) \end{aligned} \quad (3.11)$$

with  $K_{12}$  the global heat exchanger coefficient,  $A_{12}$  the cross-sectional area of the tube,  $T_{t1}$  and  $T_{t2}$  the temperatures of Tank 1 and Tank 2, respectively,  $T_{oe1}$  and  $T_{oe2}$ , the outlet temperatures from the exchanger. [17] The arithmetic mean generally leads to an overestimation of the power exchanged by the heat exchanger. However, if the two temperature differences,  $\Delta T_1$  and  $\Delta T_2$ , differ by less than 40% the error that would be

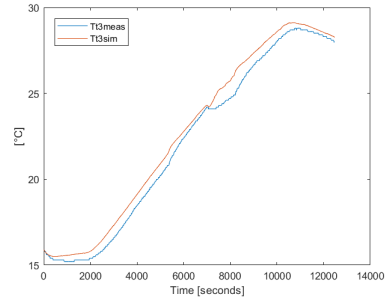
made would be less than 1%. To have an additional confirmation of the choice made, a verification test was performed by substituting the NTU method with the arithmetic mean. As can be seen from the graphs in Figure 3.3, despite the approximation the predictive model well represent the real temperature trends measured on the plant.



(a) Temperature  $T_{T1}$ : Predictive model vs experiments



(b) Temperature  $T_{T2}$ : Predictive model vs experiments



(c) Temperature  $T_{T3}$ : Predictive model vs experiments

Figure 3.3: Temperature trend of the predictive model and real experiments

The equations (3.10) and (3.11) are introduced as constraints, together with the other equations presented in (1.49) - (1.59) The overall model can be written as

$$\dot{X}(t) = f(X(t), U(t), D(t)) \quad (3.12)$$

To find a solution, it is convenient to express the differential equations in discrete time. The temperature of the flow rate leaving the secondary heat exchanger,  $T_{heu}$ , is already defined with a discrete-time model; in fact, as already seen, the load was identified with an ARX model. So, to obtain a discretized model, the Euler Forward (EF) method was used, leading to

$$X(k+1) = X(k) + \tau \cdot f(X(t), U(t), D(t)) \quad (3.13)$$

where  $\tau$  is the sampling time used to discretize the model, where  $\tau = 20sec$  given that the ARX model since the ARX model was identified with a sampling period of, precisely, 20 seconds.

### 3.3.2. Simulation

After the problem formulation was defined and implemented in the software, an initial simulation was performed. The input and states constraints are:

**Inputs Constraints**

	min Value	max Value
$u_1$	0	2200
$u_2$	1/3600	399/3600
$u_3$	1/3600	399/3600
$\delta u_1$	-1000	1000
$\delta u_2$	-300/3600	300/3600
$\delta u_3$	-300/3600	300/3600

**Table 3.1:** Constraints on the Inputs and Inputs variation. The value for the flow rates, since in the model are used in  $[\frac{Kg}{s}]$  is reported its conversion from  $[\frac{l}{h}]$ .

**States Constraints**

	min Value	max Value
$x_1$	0.05	1
$x_2$	0.05	1
$x_3$	5	80
$x_4$	5	80
$x_5$	5	80

**Table 3.2:** Constraints on the states

In these experiments, a prediction horizon of 30 samples,  $N = 30$ , and the MPC execution period of 20 seconds, so a prediction time window of 600[s], that is, 10 minutes, were



considered. The  $Q$  and  $R$  matrices are defined as:

$$\mathbf{Q} = \begin{bmatrix} 10^{-8} & 0 & 0 & 0 & 0 \\ 0 & 10^{-8} & 0 & 0 & 0 \\ 0 & 0 & 1 & 0 & 0 \\ 0 & 0 & 0 & 1 & 0 \\ 0 & 0 & 0 & 0 & 10^{-8} \end{bmatrix} \quad \mathbf{R} = \begin{bmatrix} 1 & 0 & 0 \\ 0 & 1 & 0 \\ 0 & 0 & 1 \end{bmatrix} \quad (3.14)$$

The choice of weights lies in the fact that the values of interest are only the temperature of Tank 1 and that of Tank 2, that is the third and fourth state and therefore the others have been assigned very low weights. The following results were obtained through simulations

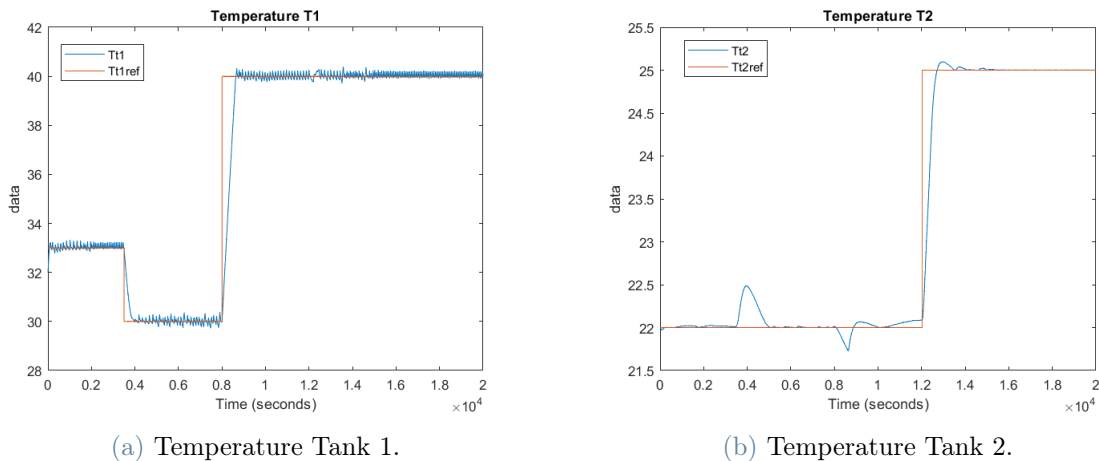


Figure 3.4: Simulation test: Temperature trends of the first simulation test

From this first experiment it can be well seen that the temperature of Tank 1 follows the reference very well, and its behavior is not nearly affected by changes in the secondary. As for  $T_{t2}$ , this follows the reference well, but is greatly influenced by changes in the primary temperature reference which cause large spikes in the trends, as can be clearly seen in Figure 3.4b. To solve this problem, or at least reduce the amplitude of these spikes, it is decided to weight more the error of the difference between the acquisition and the temperature reference of Tank 2 compared with Tank 1.

It is also important, however, to analyze the behavior of the control variables. In Figure 3.5, the trends of the flow rates control variables are shown.

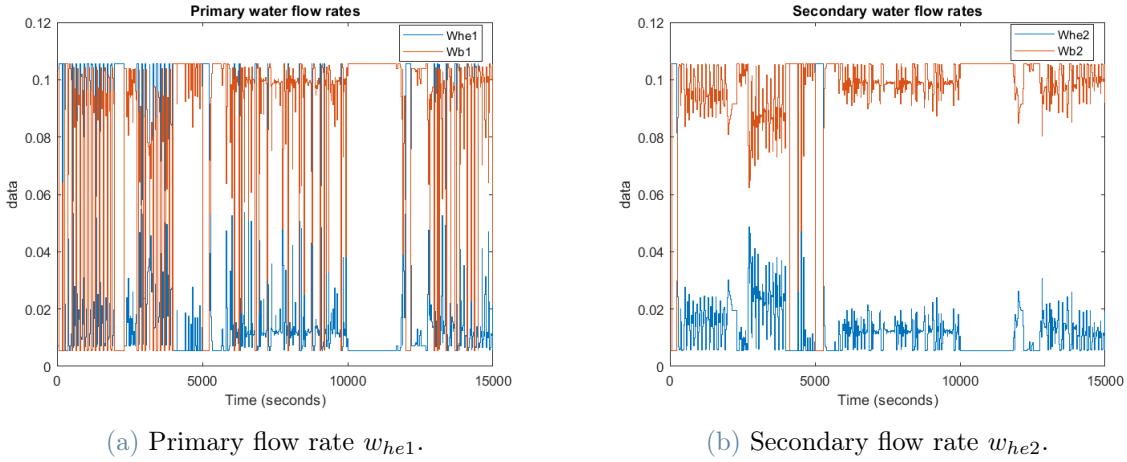


Figure 3.5: Simulation test: Water flow rates passing through the primary heat exchanger in the case of  $R$  identity matrix

As can be seen from Figures 3.5a and 3.5b, the flow rates also vary greatly from step to step, even changing from the minimum value to the maximum value or vice versa. However, this cannot coincide with the actual behavior of the variables, because the valves have their own dynamics and the set-point value is not reached immediately but with some delay. In addition, such frequent variation in control action would lead to increased actuator deterioration. Thus, remembering the cost function, to obtain a control action with less variation one changes the weights of the  $R$  matrix. In fact, the latter weights the quadratic error between two successive input sequences. Remember also that the three control variables have different orders of magnitude, i.e., the electric power  $P_e$  varies between a minimum of 0 and a maximum of 2200, while the two flow rates,  $w_{he1}$  and  $w_{he2}$ , between 0 and 0.111. Because of these reasons it was decided to change the  $R$  matrix so as to normalize these quantities so as to weigh more the variations of flow rates. The matrices  $Q$  and  $R$  become:

$$\mathbf{Q} = \begin{bmatrix} 10^{-8} & 0 & 0 & 0 & 0 \\ 0 & 10^{-8} & 0 & 0 & 0 \\ 0 & 0 & 1 & 0 & 0 \\ 0 & 0 & 0 & 10 & 0 \\ 0 & 0 & 0 & 0 & 10^{-8} \end{bmatrix} \quad \mathbf{R} = \begin{bmatrix} 10^{-3} & 0 & 0 \\ 0 & 10^5 & 0 \\ 0 & 0 & 10^5 \end{bmatrix} \quad (3.15)$$

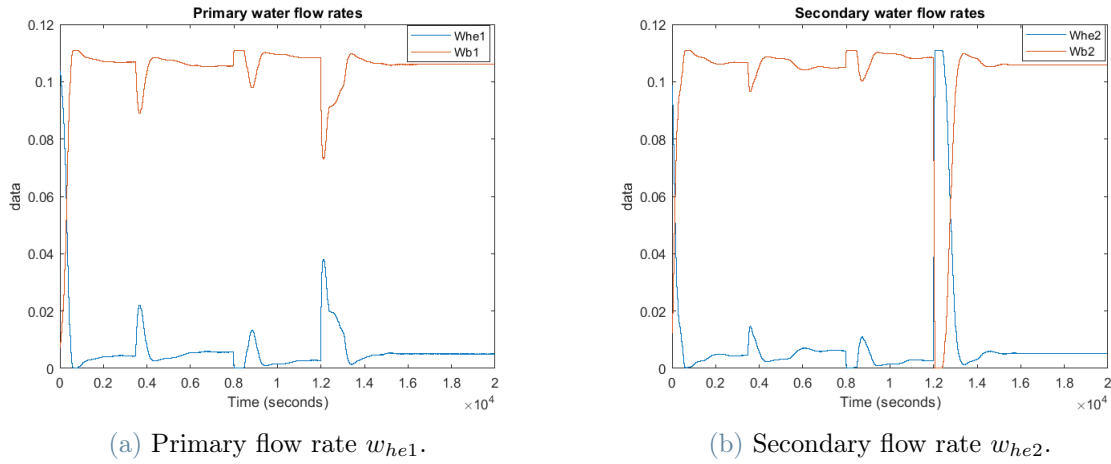


Figure 3.6: Simulation test: Water flow rates passing through the primary heat exchanger with Q and R matrices in (3.15).

Figure 3.6 shows the trend of the control variables  $w_{he1}$  and  $w_{he2}$  with the new R matrix. As can be seen, now the two rates no longer change value significantly, but the variation between steps remains small. The graphs with new temperature trends are shown in Figure 3.7. In Figure 3.8, instead, the values of the electric power are reported, it should be remembered that these are the results of optimization and then the set-point values that are then managed by the heater with the PWM modulation to obtain the desired average value.

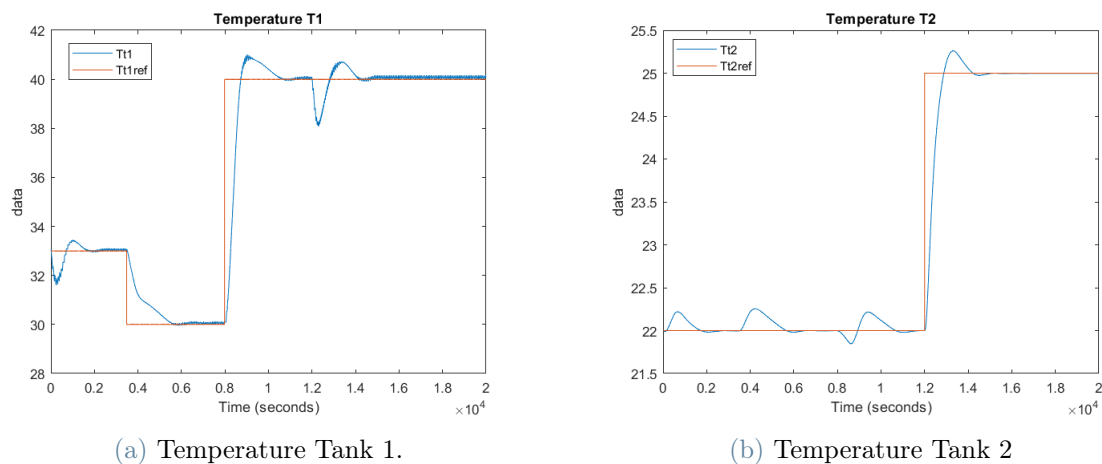


Figure 3.7: Simulation test: Temperature trends with Q and R matrices in (3.15).

In Figure 3.7 are shown the two temperature tracking for the same scenario as before. As can be seen there are no significant differences with the previous trends, and the references

continue to be followed in satisfactory manners.

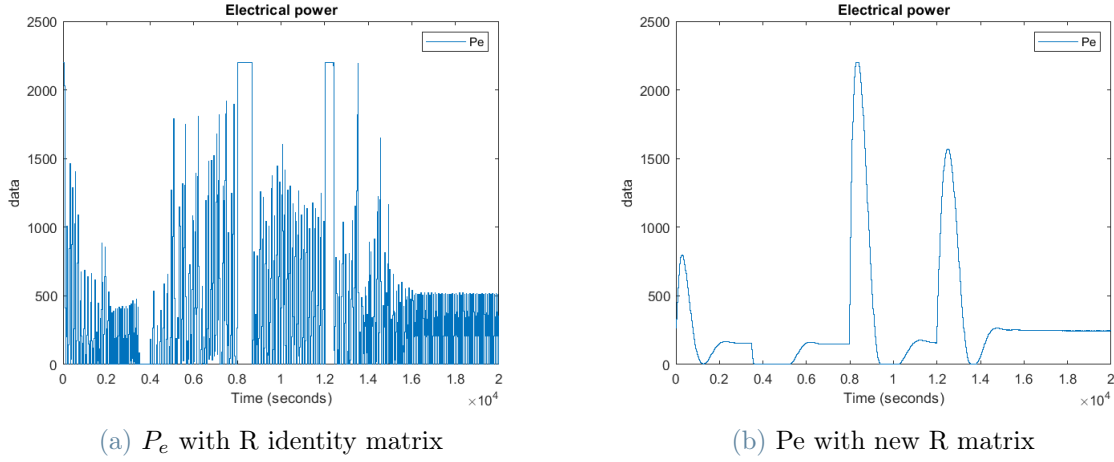


Figure 3.8: Simulation test: Comparison of  $P_e$  control variables.

Figure 3.8 compares the setpoint values of electrical power in the two simulations, on the left with R identity matrix, Figure 3.8a, on the right, Figure 3.8b, the R matrix defined in (3.15). As can be clearly seen the two trends are very different, in the first test the power varies between minimum and maximum values at almost every step, thus causing non-optimal power usage, while balancing the weights of the variations between one input and the next, leads to a power trend with no more oscillations .

### 3.4. MPC Complexity Reduction

The main disadvantage of MPC-type control is computational time; in fact, at each step time an optimization problem is solved that also is based on predicting the system's behavior over a time horizon. Since the process under consideration is a thermal process, the dynamics is quite slow, so it is not worth considering such a small prediction window (i.e., 10 min). Increasing the prediction horizon, however, would lead to an increase in computational time. Finding techniques that speed up optimization is the main challenge with regard to predictive controls. As mentioned earlier, hardware development over the years has led to reducing this time by expanding the fields of use, such as in the automotive field. However, this is not enough, so other strategies must be employed. One of these is reducing the number of controlled variables, that is, limiting this number can reduce the complexity of the optimization problem and speed up the calculation. In fact, in a FHOCP its complexity depends on its number of degrees of freedom, which corresponds to the number of inputs  $m$  multiplied by the predictive horizon  $N$ . In order to reduce

this complexity, the so-called "Input Blocking" (IB) strategy has been implemented, also called move blocking strategy [3].

### 3.4.1. Input Blocking (IB)

Since the objective is to increase the prediction time window  $N$ , it is common practice to reduce the degrees of freedom by fixing the input to be constant over several time-steps. In this way, instead of solving the optimal problem (3.4) with respect to the input sequence  $U = [U_0, \dots, U_{N-1}]$ , the new problem can be restated in terms of solving for the optimal vector  $\hat{U} = [\hat{U}_0, \dots, \hat{U}_{v-1}]$  with  $v < N$ , number of input blocks. In addition to the complexity reduction, the choice to generate the control variables and keep them constant for a larger time window than the sampling time is also due to the system dynamics being quite slow and therefore it does not make sense to generate them every 20 sec. To recap, first a predictive horizon,  $N$ , is chosen, then the number of input blocks  $v$  is found through the choice of  $N_b$ , which is the number of instants for which the control is to be kept constant, indeed  $v = \lfloor \frac{N}{N_b} \rfloor$ , finally the MPC execution period is calculated as  $N_b \cdot \tau$ . So in order to keep constant the input value during the prediction routine while the other variables vary, its index is defined as

$$u(i) = \hat{u}(\lfloor i/N_b \rfloor), \quad i = 0, \dots, N - 1 \quad (3.16)$$

and so the new NMPC formulation becomes

$$\begin{aligned} & \underset{\hat{U}}{\text{minimize}} && \sum_{i=0}^{N-1} \|x(i+1|k) - x^{ref}\|_Q^2 + \sum_{j=0}^{v-1} \|\Delta \hat{u}(j+1|k)\|_R^2 + \rho s \\ & \text{subject to} && x(i+1|k) = f(x(i|k), u(i|k)), \quad i = 0, \dots, N - 1, \\ & && u(i|k) = \hat{u}(\lfloor i/N_b \rfloor |k), \quad i = 0, \dots, N - 1, \\ & && x(0|k) = x_0, \\ & && U_{min} \leq U(k) \leq U_{max}, \\ & && \delta U_{min} \leq \Delta U(k) \leq \delta U_{max}, \\ & && X_{min} - sI \leq X(k) \leq X_{max} + sI, \\ & && s \geq 0 \end{aligned} \quad (3.17)$$

As already seen, choosing a number of input variables too large would not make sense and increase the complexity, but also choosing a long period of time in which the input value remains constant would not lead to satisfactory control action. The right trade-off

must be found between a long enough prediction horizon in order to capture the entire dynamics, a smaller number of input blocks so as to reduce the complexity of the system but also not too few to be able to generate the control actions efficiently.

Several simulations were then carried out with the choice of different parameters with the goal of finding the best choice based on performance and computational time.

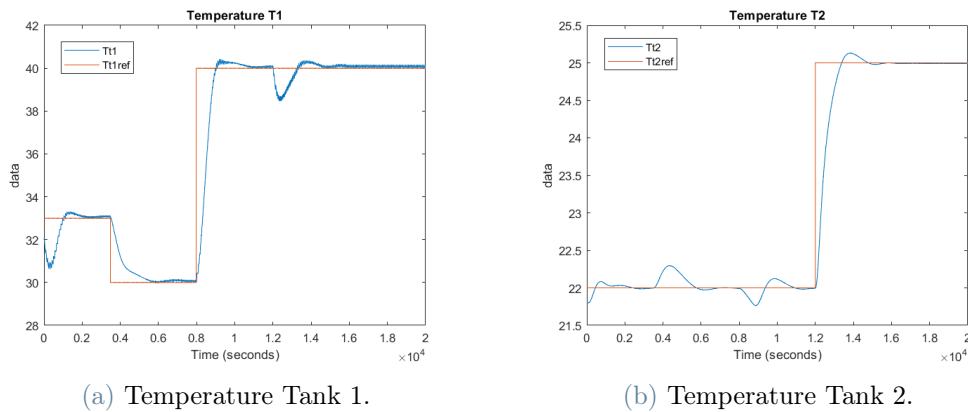


Figure 3.9: Simulation test: Tracking Reference with  $N=60$  and  $N_b = 3$ , so the input remains constant for 1 min

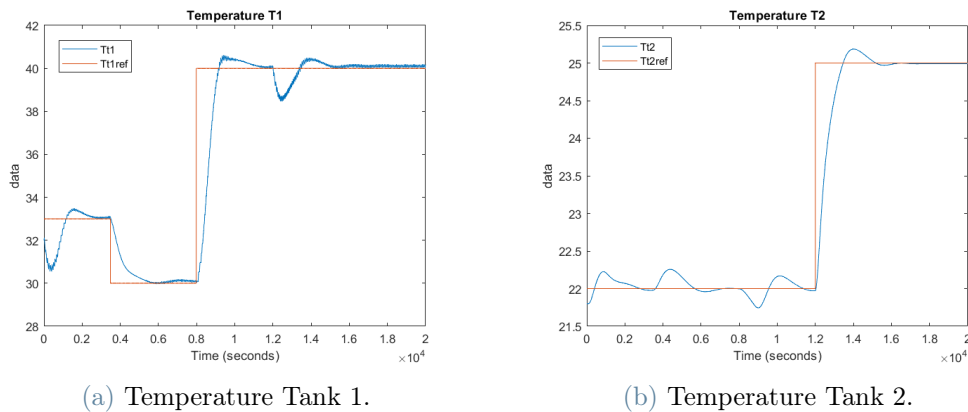


Figure 3.10: Simulation test: Tracking Reference with  $N=60$  and  $N_b = 6$ , so the input remains constant for 2 min

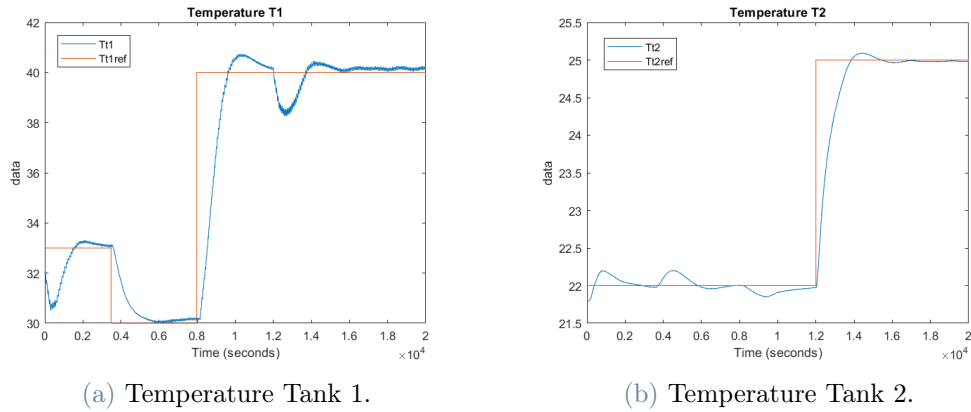


Figure 3.11: Simulation test: Tracking Reference with  $N=90$  and  $N_b = 15$ , so the input remains constant for 5 min

The above figures show the tests in simulations with the different parameters, specifically the test in Figure 3.9 generates control variables every minute, while in the second, Figure 3.10, they are generated every two minutes and in the last one, Figure 3.11, every 5 min. Obviously, the test with the shorter MPC execution period has a better performance than the other two, but since the trends are quite similar and being a system with slow dynamics, choosing to hold the values of the inputs constant for 5 minutes may be a reasonable choice because, since it has less complexity, that means less computational time and also allows to increase the predictive horizon.





# 4 | MPC Implementation in the real system

The main peculiarity of this work, as it has already been mentioned, is the possibility of testing the designed control choices made in simulation on the real plant. In the next section, the experimental system scheme is described in the following, explain it in more detail by illustrating all the components.

## 4.1. Test Plant

In Figure 4.1 is shown again a photo of the plant present in IRMAP laboratory. One can easily distinguish the two hydraulic circuits, in fact the primary as already mentioned is thermally insulated and in the photo it is distinguished by the fact that its components, i.e., Tank 1 and pipes, are coated, on the right black coating. Whereas, on the left you can see the secondary components without coatings and in particular on the top left there is Tank 3 and in the center of the photo Tank 2. It is also possible to note the computer with which the communication and interface between PLC and Matlab is handled for the acquisitions of measurements from the sensors and the generation of the control variables. Thanks to the use of remote control software, it is possible to connect remotely to the PC that manages the control of the system to perform and monitor the tests and therefore without the need to be present on the plant. Everything related to sensing and low-level control is the result of previous work on the plant and a general description will be given in this chapter.

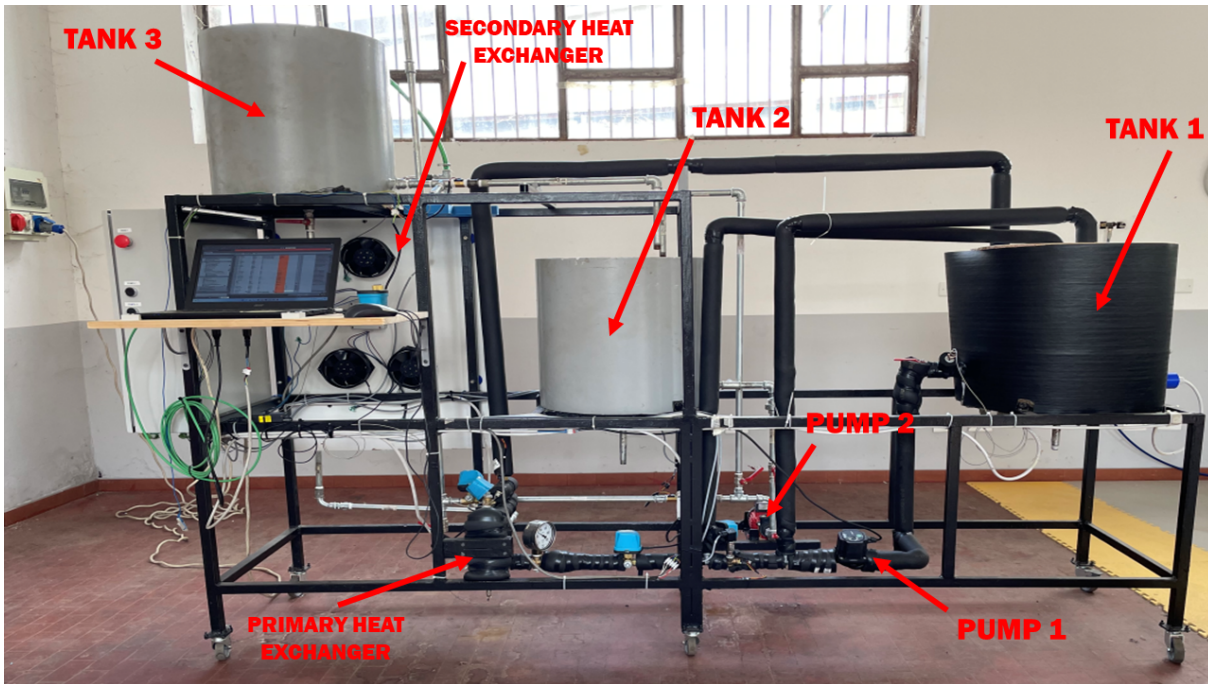


Figure 4.1: Test Plant

The test plant is located over a structure made of welded steel components and on its legs are welded plastic wheels to move the structure easily. The piping are made of 1/2" G galvanised steel pipe, standard model for industrial applications EN10255, and cast iron fittings according to ISO-EN 10242. The three tanks are made of 3-mm-thick sheet steel, arc-welded and painted on the inside surface with water-resistant paint, they have a diameter and a height of 50[cm]. In the primary circuit tank, Tank 1, there is a submerged electrical resistor.

## 4.2. Components

Taking the total schematic of the plant (1.1), it is possible to distinguish the different sensors and actuators present, which will be explained in more detail below. First, however, it is appropriate to start with the component that is responsible for managing all the devices, namely the Programmable Logic Controller (PLC).

### 4.2.1. Programmable Logic Controller

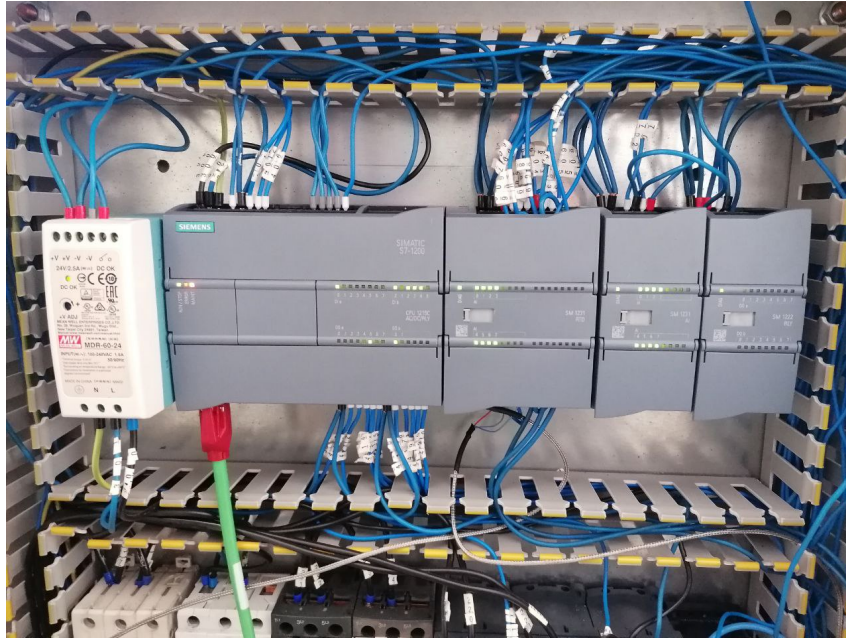


Figure 4.2: SIEMENS PLC S7-1200

The PLC used is a SIEMENS PLC S7-1200. To connect the PLC and program on it, the Totally Integrated Automation(TIA) Portal by Siemens is used. The TIA Portal is basically a centralized design environment featuring a common user interface for all automation tasks, and in fact thanks to it, all quantities such as temperatures and flow rates can also be monitored during testing. Its main functions are the following:

- Data acquisition from sensors and filtering action.
- Interfacing with Matlab.
- PWM modulation.
- Implementation of low-level control architectures.

Functions are also listed according to the order with which they are performed. So starting with the first function what the PLC does is to take the values provided by the sensors, which can be both analog and digital signals, applies a filtering and conversion action so that values with the desired order of magnitude are obtained, then sends the filtered values to Matlab. Control variables are generated according to a given control action and sent to the PLC, which controls the actuators to get the desired values. In addition, as already explained, the PLC also performs PWM modulation of the power to be provided

to the resistor present in Tank 1. A schematization of the flow of information exchanged throughout the system is shown in Fig.(4.3).

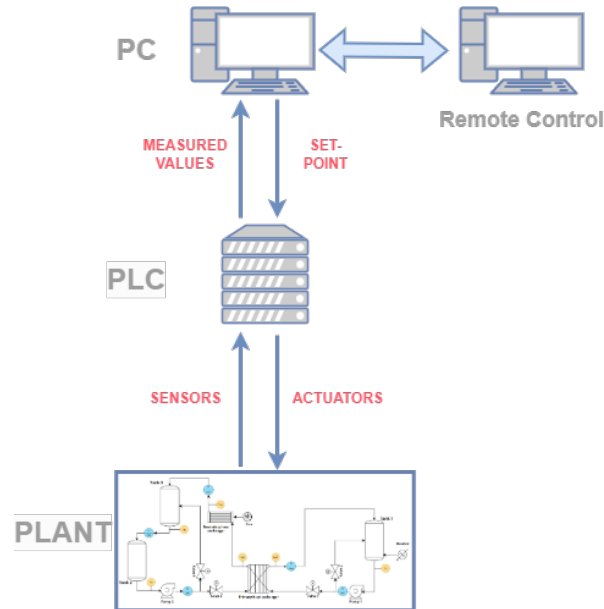


Figure 4.3: General scheme of the connection and flow of information of the entire system

## 4.2.2. Sensors

### Flow Meters

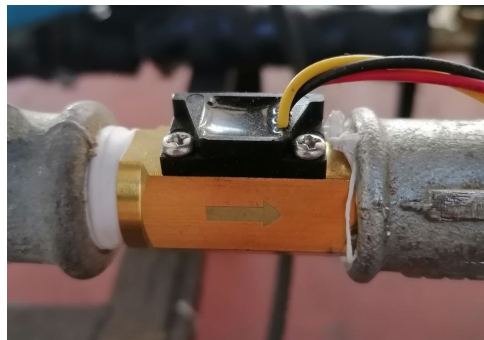


Figure 4.4: Flow Meters

There are five flow meters present and they measure the main flow-rates of interest, i.e., the two flow rates passing through the primary exchanger, the flow-rates of the two pumps, and finally the flow-rate passing between Tank 3 and Tank 2.

The sensor is a turbine flow meter, its working principle is very simple, in fact inside the sensor there is a turbine that is set into rotation by the kinetic energy of the flow.

The central element, the rotor, with the splined vanes then rotates with a frequency proportional to the flow rate, that is, the rotation speed is linear to the flow rate. For counting the number of turns there is a permanent magnet that sends a pulse each passage of the vane, so the formula for calculating the flow rate is as follows:

$$W = k \cdot rpm \quad (4.1)$$

Where  $W$  is the flow rate in  $[\frac{l}{h}]$ ,  $k$  constant of proportionality specific to each turbine and  $rpm$  the numbers of rotations. The constant  $k$  is calculated through calibration of the flow meter and is peculiar not so much to each turbine as to its rotor assembly. The formula (4.1) is performed in the PLC program which receives the number of rotations in terms of a digital signal and then, being a very noisy value, as mentioned above it is filtered with a I-order filter and finally sent to Matlab.

### Temperature sensor



Figure 4.5: Resistance Temperature Detectors (RTD)

There are six temperature sensors that measure the temperature of the Tanks and of the main flow rates in the circuit, in addition, there is also a sensor that measures ambient temperature.

The Resistance Temperature Detectors (RTD), RTD PT100 are characterized by a 1/2"

stainless steel tip capable to measure temperature values ranging from  $-50^{\circ}\text{C}$  to  $300^{\circ}\text{C}$ . Being cheap sensors, they do not have great accuracy, in fact the systematic error is about  $1[^{\circ}\text{C}]$ , and several times their calibration had to be carried out. The sensors send a value to the PLC that corresponds to the recorded temperature multiplied by 10, so in the hundreds, this value is then rescaled in the desired order before being filtered and sent to Matlab.

### 4.2.3. Actuators

#### Valves



Figure 4.6: Valves. Specifically in the photo are shown the two valves that handle the bypass of the secondary circuit.

There are four valves in the plant, two per circuit. These regulate the different flows through the various pipelines. Their models are not derived since their control is not part of this discussion. But, since these flows come into play in all the balance equations, it is appropriate to explain how their regulation takes place.

The PLC, through a Matlab interface, receives the desired flow rate values. These values can be set by the user to perform experiments, or they can be the result of a control action. Either way, the flow regulation is done by adjusting the placement of the plug between the open and closed positions of the valve. The type of control implemented for each valve is a PID control in which its parameters were calculated taking into account

that each valve takes 8s to completely open from the close position and vice versa.

Another consideration can be made: it is enough to provide the setpoint of one of the two flow rates, the value of the other is found with a simple difference, since the pumps operate at their nominal conditions. In fact, as a result of optimization, i.e., as control variables, the values of the flow rates passing through the heat exchanger are obtained,  $w_{he1}$  and  $w_{he2}$ , and the desired bypass reference flow rates are calculated with the following formulas:

$$w_{b1}(t) = w_{p1}(t) - w_{he1}(t); \quad (4.2)$$

$$w_{b2}(t) = w_{p2}(t) - w_{he2}(t); \quad (4.3)$$

A schematization of the process can be represented by the scheme in the figure below.

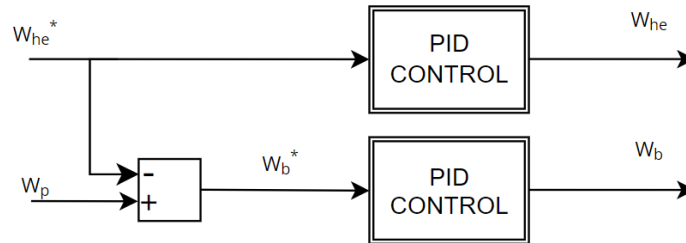


Figure 4.7: Generalized PLC program architecture for valve control. The \* sign means that the signal is a setpoint value. The flow rate value provided by Matlab is used as the setpoint in the first PID control, while, to obtain the other desired value, the difference is made with the fixed value of the pump flow rate.

## Pumps



(a) Pump 1.



(b) Pump 2.

Figure 4.8: Pumps

The two pumps present, P1 and P2, are used to circulate the water through the primary and secondary hydraulic circuits, respectively, and that is why they are kept active at all times and operate at their nominal conditions. The first one is a water circulator with self-adjusting motor and the second one is a simple centrifugal electric water pump. Since in the pumps no mass accumulation is allowed, then the mass balance comes to eq.(4.4)

$$w_{ip}(t) = w_{op}(t) \quad (4.4)$$

with  $w_{ip}(t)$  and  $w_{op}(t)$  respectively the inlet and outlet pump mass flow.

The control loop structure designed to control pump flow rates is shown in Figure 4.9.

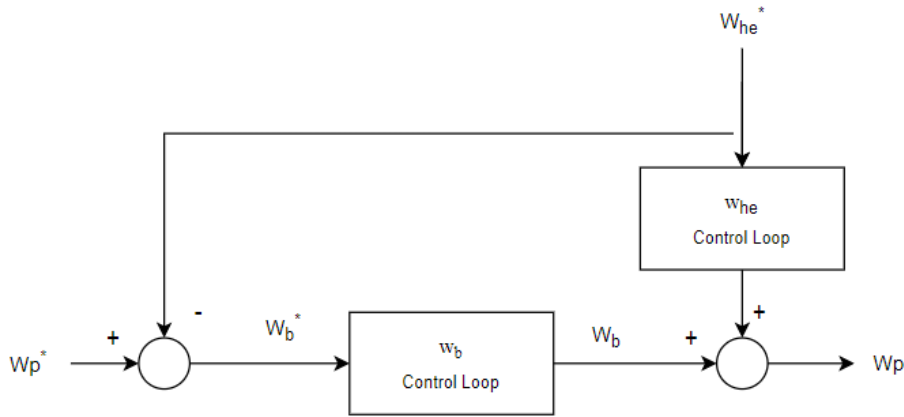


Figure 4.9:  $W_p$  flow control loop. Also in this case the \* sign means that the signal is a setpoint value. The two control loop present are the ones of the valves explained in the previous paragraph

So, in order to control  $w_{op}$ , the flow rate of the bypass,  $w_b$ , is used as a control variable while  $w_{he}$  is considered as disturbance. The control function can be state as

$$W_b^*(s) = W_{op}^*(s) - W_{he}^*(s) \quad (4.5)$$



#### 4.2.4. Secondary Heat Exchanger and Fans System



Figure 4.10: Secondary Heat Exchanger. From the picture, it can be seen the three fans mounted behind the component for additional flow cooling.

The secondary heat exchanger consists of a process component designed to decrease the outlet water temperature emulating a residential radiator. The flow rate passing through the radiator, that is, the incoming flow rate from the primary heat exchanger, is cooled by exchanging heat with the environment. There is also the presence of three fans that, when activated, increase the heat extracted from the exchanger to the room. The activation of them was initially done through a manual command, and thus the presence of an operator was required to activate and turn them off. Afterwards, it was possible, through the help of a contactor, to perform the activation and shutdown through the user interface from the PLC programming environment, i.e., TIA Portal and so remotely.

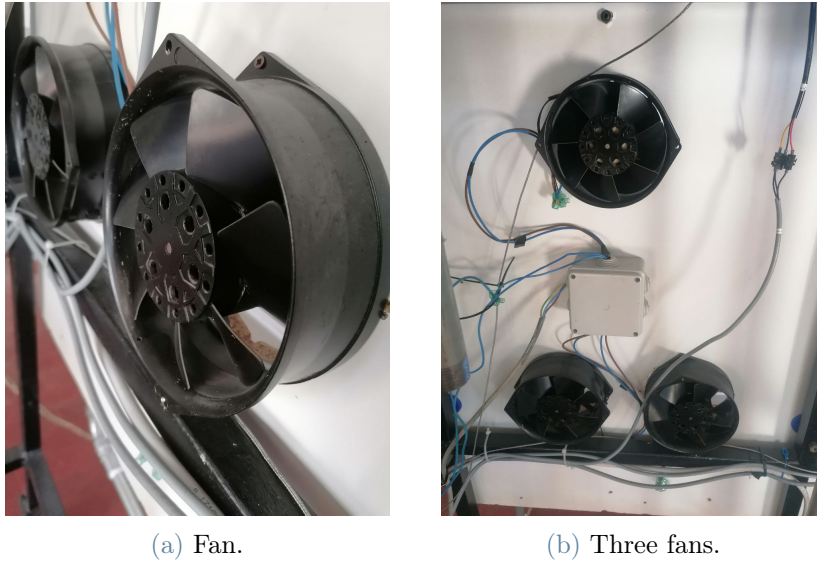


Figure 4.11: Fan system

### 4.3. Experiments

This section will illustrate and discuss the results obtained by applying the control system, designed and tested in simulation, on the real plant. However, some clarifications should be made first:

- The sensors present, thermo-couples and flowmeters, are not of very good quality and therefore their measurements are not always accurate.
- The valves also are not of the best quality, their control is not always precise, and several times they have had to be replaced due to functional problems.

#### 4.3.1. MPC control

The type of control used is the same as discussed in the previous chapter, i.e. an MPC control with Input Blocking strategy with the following parameters:  $N = 90$ ,  $Nb = 15$ , therefore the execution period of the MPC equal to 5 minutes. That is, a predictive horizon of 30[*min*] and control variables held constant for 300[*s*].

However, there are some differences to highlight compared with the simulation. First of all, the model present in the simulator provides the Tank heights of the secondary circuit as outputs, these values, which are fundamental, but they were not measured in reality as there are no sensors in the plant for this purpose. The solution found is to estimate them using equations (1.54) and (1.56) so that they can be used in the predictive model.

Therefore, the measured values of the flow rates of interest, namely  $w_{p2}$  and  $w_{t3}$ , are needed; in addition, the measurement of the flow rate  $w_{he2}$  for the ARX model of the secondary heat exchanger is also needed. As already mentioned flow meters are of low quality and provide very noisy values, using filtered data also is not even possible because there is a delay between the acquired measurement and the filtered value, so the solution found is to use as measurements the values of the control variables obtained as a result of the optimization in the previous step. On the other hand, for temperatures, being more precise measurements, the values of the acquisitions have been used. The matrices  $\mathbf{Q}$  and  $\mathbf{R}$  are the same as the one used in simulation:

$$\mathbf{Q} = \begin{bmatrix} 10^{-8} & 0 & 0 & 0 & 0 \\ 0 & 10^{-8} & 0 & 0 & 0 \\ 0 & 0 & 1 & 0 & 0 \\ 0 & 0 & 0 & 10 & 0 \\ 0 & 0 & 0 & 0 & 10^{-8} \end{bmatrix} \quad \mathbf{R} = \begin{bmatrix} 10^{-3} & 0 & 0 \\ 0 & 10^5 & 0 \\ 0 & 0 & 10^5 \end{bmatrix} \quad (4.6)$$

### Tracking Reference without fan activation

The first test performed concerns the tracking of the reference, specifically the scenario involves a first step on the temperature of Tank 1 and then another step on the temperature of Tank 2. The next two figures show the results obtained.

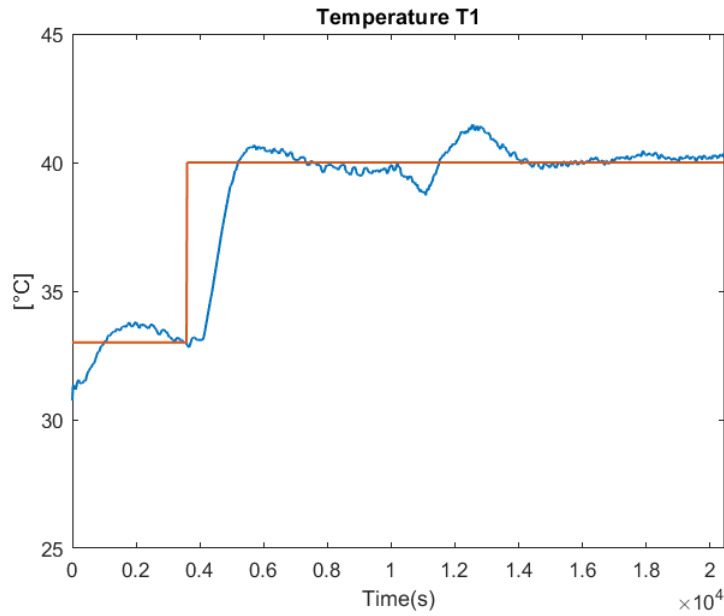


Figure 4.12: Experimental test: Temperature  $T_{t1}$  Trend

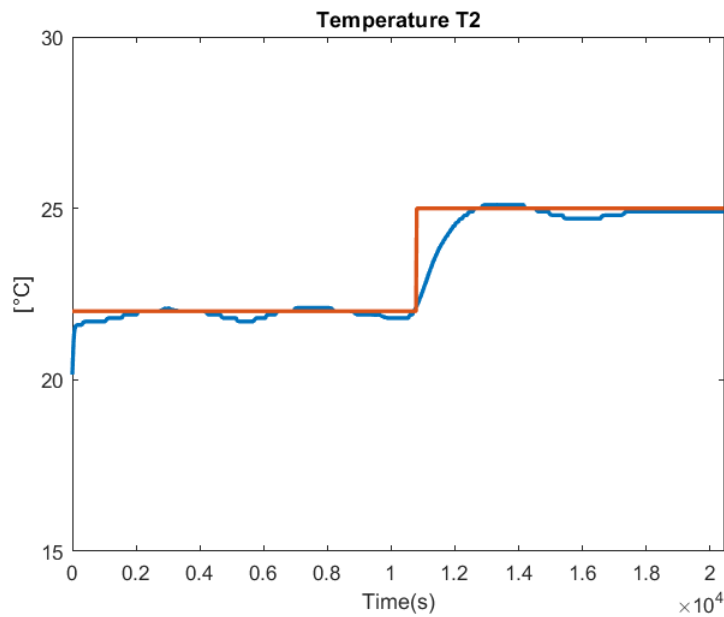


Figure 4.13: Experimental test: Temperature  $T_{t2}$  Trend

The results obtained are very satisfactory, the trends of the temperature  $T_{t1}$ , Figure 4.12, and of  $T_{t2}$ , Figure 4.13, follow the reference the reference very well, Fig. 4.13, however  $T_1$  it presents some oscillations due to the PWM modulation. As can be seen, when there is a step on the secondary, the control action causes the temperature  $T_{t2}$  to increase, in this

way it then transfers heat to the secondary by opening the valves that manage the flow going to the exchanger and  $T_{t2}$  increases, reaching the reference.

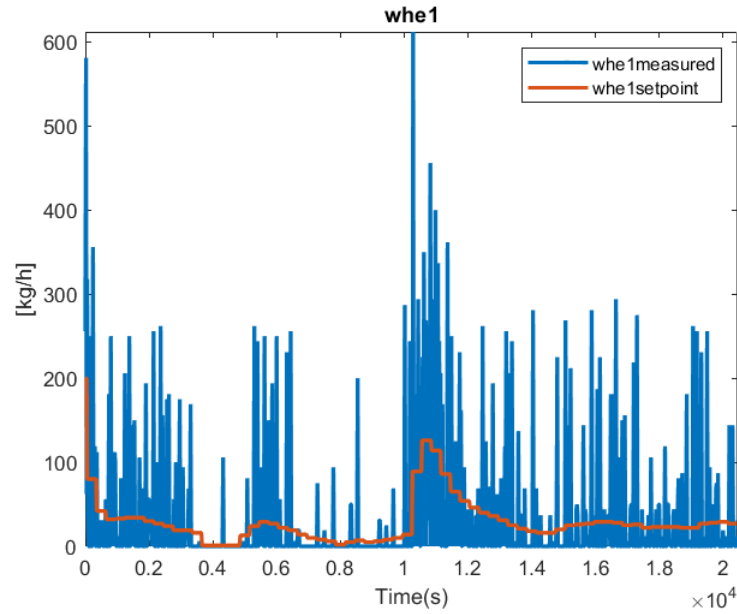


Figure 4.14: Experimental test: Control Variable  $w_{he1}$ . "whe1measured" are the values of the acquisitions not filtered; "whe1setpoint" are the setpoint for PID control

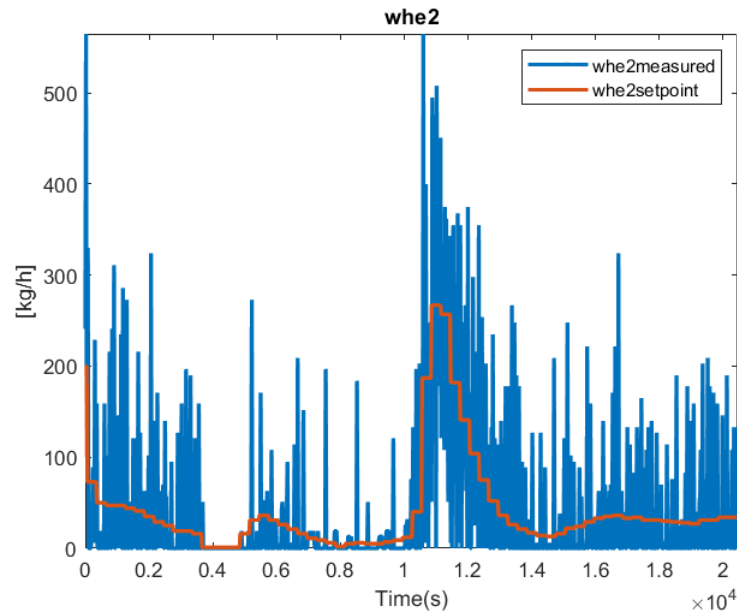


Figure 4.15: Experimental test: Control Variable  $w_{he2}$ . "whe2measured" are the values of the acquisitions not filtered; "whe2setpoint" are the setpoint for PID control

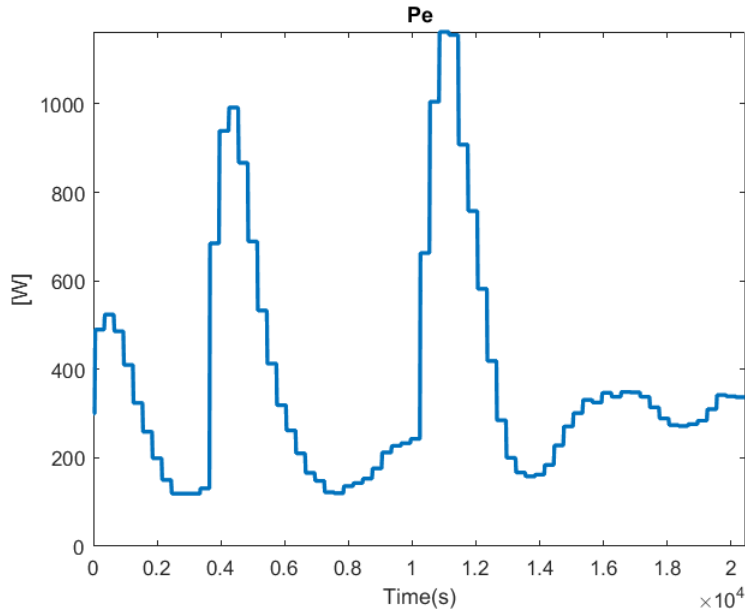
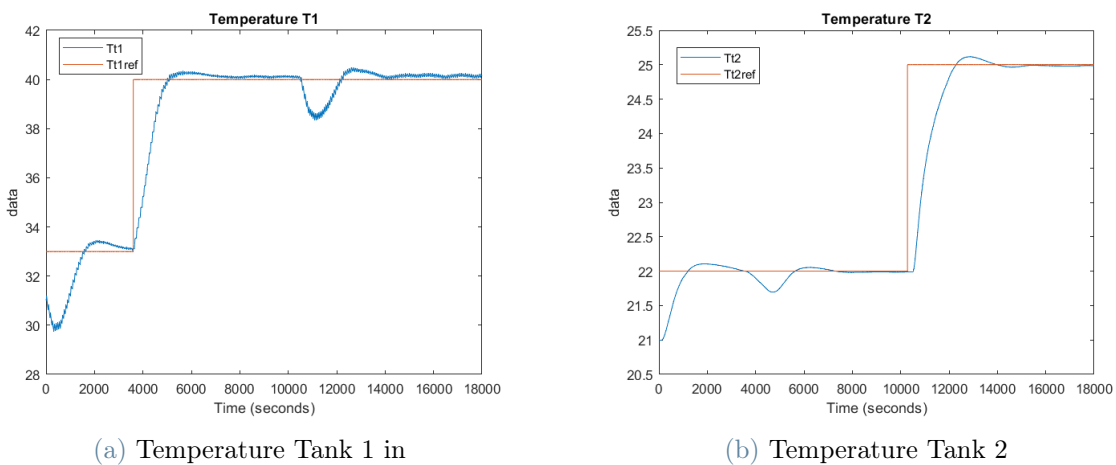


Figure 4.16: Experimental test: Control Variable  $P_e$

Figure 4.14 and 4.15 show in red the control variables, that is the values obtained from the optimization and sent to the PLC to be used as set-points in the PID controllers that manage the valves. In blue, however, are the values of the acquisitions not filtered, as it can be seen are very noisy values. The test was also performed in simulation for comparison, the result is shown in Figure 4.17. As it can be seen, the temperature trends are very similar to the real ones, confirming once again the choices made during the modelling of the whole system.



(a) Temperature Tank 1 in

(b) Temperature Tank 2

Figure 4.17: Experimental test: Temperature trends in simulation

### Tracking reference with Fan Activation

A further test was carried out with the activation of the fans for cooling the flow of water passing through the secondary heat exchanger. Thus, as mentioned above, thanks to the inserted contactor, it was possible to activate the devices even remotely without any kind of problem. The test consists to keep constant the references of the two temperatures of interest,  $T_{t1}$  and  $T_{t2}$ , turn on the fans and see how the system behaves. The fans were kept active between 3000 and 10000 seconds. In Figure 4.18 it can be seen very well how the temperature at the outlet of the exchanger during this time interval is subjected to cooling.

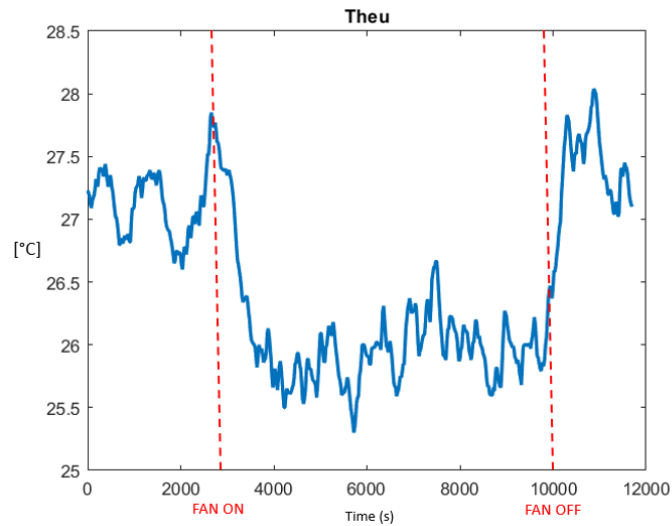
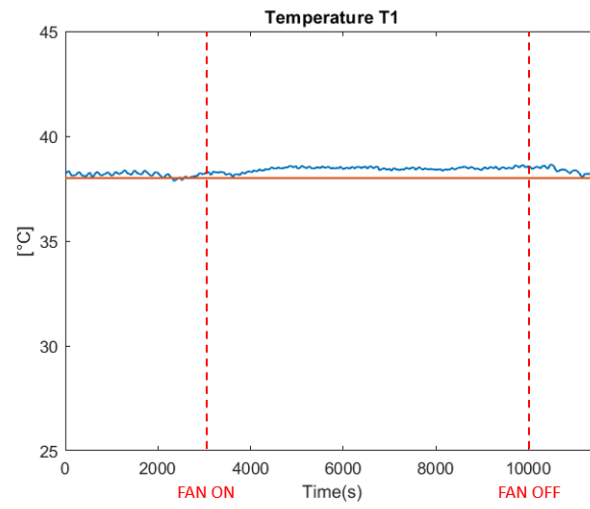
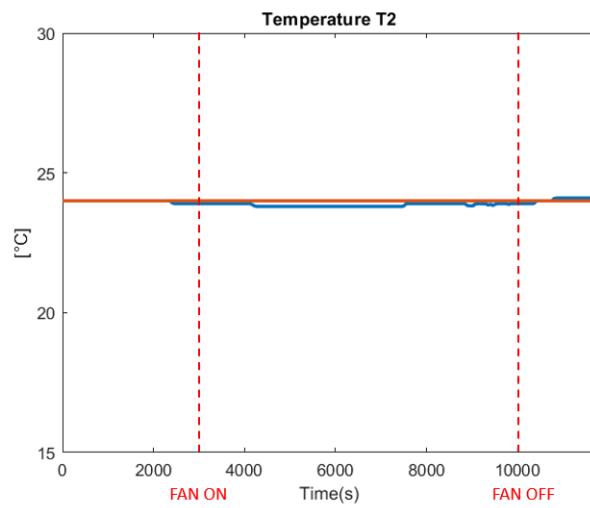


Figure 4.18: Experimental test: Temperature  $Theu$  trend with Fan activation

Instead, the next figure, Figure 4.19, shows the trends of the two temperatures and their reference. As can be seen when the fans are operated, the temperature  $T_{t2}$  decreases to a maximum difference of 0.2 degrees, and then stabilizes around a value slightly below the reference, Figure 4.19b. Instead, the control leads to an increase in  $T_{t1}$ , Figure 4.19a, as it rightly predicts a lowering of the temperature of Tank 2, and thus the primary circuit will have to give up heat to the secondary. Despite this, however, the temperatures stabilize at these values slightly different from the reference as if the control predicted a decrease in temperature in Tank 1 and an increase in Tank 2 which, however, do not occur, a cause could be due to the inaccurate identification of the ARX model of the heat exchanger with the fans on.



(a) Temperature Tank 1



(b) Temperature Tank 2

Figure 4.19: Experimental test: Temperature trends with fan activation



## Conclusions

The purpose of this thesis was to design and implement a Model Predictive Control scheme to a thermo-hydraulic plant with the aim of tracking temperature references by modulating the control variables to avoid their usage and having a better use of energy to reduce the overall costs.

One of the main ingredients of predictive control is to have a model that can predict system behavior as accurately as possible. So the first thing done was to derive the equations that govern the system starting from the physical laws, in particular the temperature dynamics of the three tanks, the water levels inside them, and the model of the heat exchangers. The secondary heat exchanger was found as ARX model with a system identification procedure.

To verify the accuracy of the modeling phase, a Simulink model of the entire plant was developed, with each of its components modeled according to the equations found. Several experiments were then performed on the real plant in order to validate the simulation model, that is, to compare the trends of significant quantities with those simulated. The results obtained were very satisfactory and allowed to be very confident to start designing the control system for the simulated model.

Since this model has nonlinearities in its formulation, it was chosen to solve a Nonlinear Model Predictive Control (NMPC) optimization problem. Several tools exist for solving these types of problems, and it was chosen to use CasADI with Ipopt as solvers because of its ease in formulating optimization problems and the ability to interface with the Matlab environment. Then given the slow dynamics of the system, to increase the predictive horizon and thus decrease the computational time of optimization, an "input blocking" strategy was introduced; hence, it was decided to generate the control variables every 5 minutes.

Finally, the control was applied and tested on the real plant; during this phase, everything related to the low-level architecture, i.e., sensors and actuators, managed by the Programmable Logic Computer (PLC) had to be fixed as well to solve some problems.

The goal of the thesis, that is, the efficiency of the system from an energy point of view by acting on the control variables, was achieved by an appropriate choice of the weights

of the Q and R matrices and by introducing a constraint on the maximum and minimum variation between one input and the next one.

In this regard, a future development could be to introduce a term that takes into account energy consumption in the cost function to be minimized or, for example, the cost of energy.

Another possible development concerns the identification of the predictive model used as a constraint in the formulation of the optimization problem, the one used in this work was derived starting from the physical laws, except the secondary heat exchanger, but, since is a nonlinear model, there are several other methods to achieve it. Having the opportunity to do experiments and thus have different data available, one can consider the system as a black-box and identify it as an Recursive Neural Networks (RNN).

## Bibliography

- [1] F. Allgöwer, R. Findeisen, and Z. Nagy. Nonlinear model predictive control: From theory to application. *J. Chin. Inst. Chem. Engrs*, 35:299–315, 05 2004.
- [2] J. A. E. Andersson, J. Gillis, G. Horn, J. B. Rawlings, and M. Diehl. CasADi – A software framework for nonlinear optimization and optimal control. *Mathematical Programming Computation*, 11(1):1–36, 2019. doi: 10.1007/s12532-018-0139-4.
- [3] R. Cagienard, P. Grieder, E. Kerrigan, and M. Morari. Move blocking strategies in receding horizon control. *Journal of Process Control*, 17(6):563–570, 2007. ISSN 0959-1524. doi: <https://doi.org/10.1016/j.jprocont.2007.01.001>. URL <https://www.sciencedirect.com/science/article/pii/S0959152407000030>.
- [4] M. Diehl. *Lecture Notes on Numerical Optimization*. Leuven-Freiburg, 2007-2016. URL [https://www.syscop.de/files/2015ws/numopt/numopt\\_0.pdf](https://www.syscop.de/files/2015ws/numopt/numopt_0.pdf).
- [5] L. M. Fagiano. "*CNOEC: Constrained Numerical Optimization for Estimation and Control*" *Lecture notes*. Politecnico di Milano.
- [6] B. Foss and T. A. N. Heirung. *Merging Optimization and Control*. 03 2016. ISBN 978-82-7842-201-4.
- [7] P. Friedlingstein, M. O’Sullivan, I. Luijkx, A. Olsen, G. Peters, W. Peters, J. Knauer, J. Korsbakken, P. Landschützer, H. Lefèvre, N. Tsujino, F. Tubiello, A. Walker, R. Wanninkhof, C. Whitehead, A. Willstrand, R. Wright, W. Yuan, C. Yue, S. Zaehle, J. Zeng, and B. Zheng. Global carbon budget 2022. *Earth Syst. Sci.*, page 4811–4900, 2022.
- [8] D. S. L. and H. C. A. *Fluid Mechanics and Thermodynamics of Turbomachinery*. Elsevier Inc, 7 edition, 2014.
- [9] A. La Bella and A. Del Corno. Optimal management and data-based predictive control of district heating systems: The novate milanese experimental case-study. *Control Engineering Practice*, 132:105429, 2023. ISSN 0967-0661. doi: <https://doi.org/10.1016/j.conengprac.2023.105429>.

[//doi.org/10.1016/j.conengprac.2022.105429](https://doi.org/10.1016/j.conengprac.2022.105429). URL <https://www.sciencedirect.com/science/article/pii/S096706612200260X>.

- [10] L. Ljung. *System Identification: Theory for the User*. PTR Prentice Hall, Upper Saddle River, NJ, 2 edition, 1999.
- [11] L. Magni and R. Scattolini. *Advanced and multivariable control*. Pitagora, 2014.
- [12] H. A. Navarro and L. C. Cabezas-Gómez. Effectiveness-ntu computation with a mathematical model for cross-flow heat exchangers. *Brazilian Journal of Chemical Engineering*, 24(Braz. J. Chem. Eng., 2007 24(4)):509–521, Oct 2007.
- [13] P. A. Nikrityuk. *Computational Thermo-Fluid Dynamics*. WILEY-VCH Verlag GmbH Co. KGaA, 1 edition, 2011.
- [14] S. Paardekooper, R. Lund, B. Mathiesen, M. Chang, U. Petersen, L. Grundahl, A. David, J. Dahlbæk, I. Kapetanakis, H. Lund, N. Bertelsen, K. Hansen, D. Drysdale, and U. Persson. *Heat Roadmap Europe 4: Quantifying the Impact of Low-Carbon Heating and Cooling Roadmaps*. Aalborg Universitetsforlag, Oct. 2018.
- [15] S. V. Raković and W. S. Levine. *Handbook of Model Predictive Control*. Birkhäuser Cham, 1 edition, 2019. doi: <https://doi.org/10.1007/978-3-319-77489-3>.
- [16] D. D. Vincenzo. La transizione energetica nell’attuale contesto globale. *Rivista geografica italiana*, pages 81–105, 3 2022.
- [17] Y. A. Çengel. *Termodinamica e trasmissione del calore*, chapter 15, pages 533–570. The McGraw-Hill Companies srl, 1 edition, 1998.

## List of Figures

1	Test Plant located at IRMAP Laboratory . . . . .	2
2	Control Scheme . . . . .	3
1.1	Scheme of the plant . . . . .	5
1.2	Scheme of the Primary circuit . . . . .	6
1.3	Scheme of Secondary circuit . . . . .	7
1.4	Tank 1 schematic . . . . .	12
1.5	Primary heat exchanger schematic . . . . .	15
1.6	Tank 2 schematic . . . . .	17
1.7	Tank 3 schematic . . . . .	19
1.8	Secondary Heat Exchanger schematic . . . . .	21
2.1	Simulink model of the plant . . . . .	27
2.2	Tank 1 simulation model . . . . .	28
2.3	Heater simulation model . . . . .	29
2.4	Primary Heat Exchanger with NTU method simulation model . . . . .	30
2.5	Secondary Circuit simulation model . . . . .	30
2.6	Tank 2 simulation model . . . . .	31
2.7	Tank 3 simulation model . . . . .	32
2.8	Secondary Heat Exchanger simulation model . . . . .	33
2.9	arx model best fits . . . . .	35
2.10	Comparison of the three measured temperatures with simulated temperatures. . . . .	37
2.11	Comparison of the three measured temperatures with simulated temperatures with convection losses included. . . . .	38
2.12	Test with Fan activation 1 . . . . .	39
2.13	Test with Fan activation 2 . . . . .	39
3.1	Graphic representation of Receding Horizon principle [5]. . . . .	42
3.2	Simulink model used for MPC control . . . . .	45
3.3	Temperature trend of the predictive model and real experiments . . . . .	47

3.4	Simulation test: First Tracking . . . . .	49
3.5	Simulation test: Control Variables Flow Rates First simulation . . . . .	50
3.6	Simulation test: Flow rates with new Q and R matrices in simulation . . . . .	51
3.7	Simulation test: Temperature trends with the new matrix R. . . . .	51
3.8	Simulation test: Comparison of Pe control variables in simulation . . . . .	52
3.9	Simulation test: Tracking Reference with N=60 and Nb = 3 . . . . .	54
3.10	Simulation test: Tracking Reference with N=60 and Nb = 6 . . . . .	54
3.11	Simulation test: Tracking Reference with N=90 and Nb = 15 . . . . .	55
4.1	Test Plant . . . . .	58
4.2	PLC . . . . .	59
4.3	System connection . . . . .	60
4.4	Flow Meters . . . . .	60
4.5	Thermo-couples . . . . .	61
4.6	Valves . . . . .	62
4.7	Valves PID Control Scheme . . . . .	63
4.8	Pumps . . . . .	63
4.9	$W_p$ flow control loop . . . . .	64
4.10	Secondary Heat Exchanger . . . . .	65
4.11	Fan system . . . . .	66
4.12	Experimental test: Temperature $T_{t1}$ Trend MPC Plant . . . . .	68
4.13	Experimental test: Temperature $T_{t2}$ Trend MPC Plant . . . . .	68
4.14	Experimental test: Control Variable $w_{he1}$ MPC Plant . . . . .	69
4.15	Experimental test: Control Variable $w_{he2}$ MPC Plant . . . . .	69
4.16	Experimental test: Control Variable Pe MPC Plant . . . . .	70
4.17	Experimental test: Temperature trends in simulation . . . . .	70
4.18	Experimental test: Temperature Theu trend with Fan activation . . . . .	71
4.19	Experimental test: Temperature trends with fan activation Real Plant . . . . .	72

## List of Tables

3.1	Constraints on the Inputs and Inputs variation. . . . .	48
3.2	Constraints on the states . . . . .	48





## Ringraziamenti

Desidero innanzitutto ringraziare il Prof. Alessio La Bella per il supporto e l'immensa pazienza avuti durante tutto questo progetto, incoraggiandomi e aiutandomi sempre nei momenti di difficoltà con i suoi indispensabili consigli. Ringrazio il Prof Riccardo Scatolini per la fiducia e l'opportunità concessami con questo lavoro di tesi e infine un grande ringraziamento a l' Ing. Andrea Cataldo per la disponibilità ed il suo aiuto, ma soprattutto per la sua capacità di trasmettermi passione e interesse per questo lavoro.

Volevo inoltre ringraziare i miei genitori e la mia famiglia per avermi sempre supportato durante tutto il mio percorso nascondendo gli sforzi e i sacrifici fatti per darmi la possibilità di raggiungere questo risultato. Alla mia ragazza Sara, che, oltre ad avermi sempre supportato, mi ha anche, forse di più, sopportato durante tutti questi anni a cui un grazie non basterebbe.

Infine ringrazio gli amici di sempre, i compagni di università e gli amici incontrati in Erasmus.

